TOPICAL REVIEW

Disorder effects in diluted magnetic semiconductors

Carsten Timm

Institut für Theoretische Physik, Freie Universität Berlin, Arnimallee 14,
D-14195 Berlin, Germany

E-mail: timm@physik.fu-berlin.de

Abstract
In recent years, disorder has been shown to be crucial for the understanding of diluted magnetic semiconductors. Effects of disorder in these materials are reviewed with the emphasis on theoretical works. The types and spatial distribution of defects are discussed. The effect of disorder on the intimately related transport and magnetic properties are considered from the viewpoint of both the band picture and the isolated-impurity approach. Finally, the derivation and properties of spin-only models are reviewed.

(Some figures in this article are in colour only in the electronic version)

Contents

1. Introduction

Diluted magnetic semiconductors (DMSs) are promising materials for applications as well as interesting from the basic-physics point of view. Possible applications exist in spin electronics (*spintronics*) [1, 2], which employ the spin degree of freedom of electrons in addition to their charge. This may allow the incorporation of ferromagnetic elements into semiconductor devices, and thus the integration of data processing and magnetic storage on a single chip. Since the electronic spin is a quantum mechanical degree of freedom, quantum interference effects could be exploited in devices, eventually leading to the design of quantum computers [3].

DMSs also pose a number of questions of fundamental interest for condensed-matter physics: what is the nature of disorder? What role does it play in transport and magnetism? What is the interplay between disorder physics and strong correlations? What is the mechanism of ferromagnetic ordering? What is the interplay between transport and magnetic properties? The present topical review concentrates on the first two questions. A lot of work has been done on disorder effects in nonmagnetic semiconductors and metals [4–6]. Only during the last few years have disorder effects in DMSs been considered. They can be expected to be strong due to the presence of a high concentration of charged impurities; the typical distance between these defects is roughly of the same order as the Fermi wavelength. Possibly Wan and Bhatt [7] were the first to emphasize the importance of disorder for DMSs. We here apply the term 'disorder effects' to those effects that really depend on the *random spatial distribution* of impurities and not only on their *presence*, such as the change of the carrier concentration.

This paper attempts to give an overview over present theoretical approaches for disorder in DMSs. The emphasis is on III–V materials such as GaAs and InAs doped with manganese, since these have been studied most intensively and also show promisingly high Curie temperatures. There are a number of excellent review articles covering aspects of the physics of DMSs not discussed here. Discussions of the motivation for studying DMSs drawn from possible applications can be found in [1] and [2]. Ferromagnetism in III–V materials is discussed by Ohno [8, 9] and Ohno and Matsukura [10], emphasizing experimental properties, and by Dietl and Ohno [11], discussing both experimental and theoretical aspects. The theoretical results are based on the Zener model and a mean-field approximation for the magnetic order. König *et al* [12] provide a more extensive review of theoretical results obtained by this approach. Lee *et al* [13] discuss DMS heterostructures for possible applications. It may be useful to mention the Ferromagnetic Semiconductor Spintronics Web Project at http://unix12.fzu.cz/ms/index.php. This webpage contains a large body of theoretical and experimental results and an extended bibliography. Sanvito *et al* [14] review *ab initio* calculations for III–V DMSs. Dietl [15] and Pearton *et al* [16] give overviews of ferromagnetic semiconductors not limited to diluted III–V compounds.

The remainder of this paper is organized as follows: in the rest of section 1 we first discuss basic properties of DMSs, then the types of impurity thought to be relevant and finally general consequences of the presence of magnetic impurities. In section 2 we consider the disorder more carefully, in particular the spatial distribution of impurities. Section 3 concerns the effect of disorder on transport properties and section 4 deals with disorder effects on magnetism. Finally, section 5 draws some conclusions and lists open questions.

1.1. Basic properties of DMSs

Diluted magnetic semiconductors are realized by doping a semiconducting host material with magnetic ions, typically manganese. The basic properties of DMSs depend on the type of host material: for III–V semiconductors such as GaAs, manganese plays a dual role in that it acts

as an acceptor and provides a localized spin due to its partially filled (in this case half-filled) d shell. Manganese in GaAs is in a Mn^{2+} state [17]. The doped hole is weakly bound to the acceptor by Coulomb attraction, forming a shallow impurity state split off from the valence-band top [17, 18]. The local impurity spin is coupled to the valence-band holes by exchange interaction. The shallow-impurity description probably applies since states dominated by manganese d orbitals are far from the Fermi energy [15, 17–19]. However, see [20, 21] for conflicting views. *Ab initio* theory does not yet consistently support the shallow-acceptor picture; see section 1.2. The situation for manganese in InAs, GaSb, InSb and AlSb is similar [15, 22]. On the other hand, in GaN manganese forms a *deep* acceptor, probably due to significant admixture of d orbitals [22–24].

Since manganese acts as an acceptor, manganese-doped III–V semiconductors are of p type. However, the observed hole concentration is lower than the concentration of manganese impurities due to compensation, probably by arsenic antisites (arsenic ions substituted for gallium) and manganese interstitials. Both types of defect provide electrons; i.e., they are double donors.

The experimental determination of the hole concentration is not trivial [25]. It is usually obtained from the ordinary Hall coefficient [8, 9, 25, 26], measured in a strong external field to saturate the *anomalous* Hall effect, which is due to the magnetization. But even for large fields the Hall resistivity is not linear in field. Careful analysis nevertheless finds agreement with the carrier concentration obtained independently from electrochemical profiling [25]. The Raman scattering intensity has also been used successfully to obtain the carrier density [27].

Since the equilibrium solubility of manganese is very low, III–V DMSs have to be grown under non-equilibrium conditions. Mostly molecular beam epitaxy (MBE) at low temperatures of the order of 250 °C has been used, but metallorganic vapour phase epitaxy (MOVPE) at higher temperatures has also been employed. Ferromagnetism in III–V DMSs was first found in (In, Mn)As grown by MBE [28], but the Curie temperature is low. In (Ga, Mn)As ferromagnetism above 100 K was first demonstrated by Ohno *et al* [29]. The total magnetization is dominated by the impurities because of compensation and since the impurity spins are larger ($S = 5/2$ in this case). Recently, Curie temperatures around 160 K have been reached, partly due to improved control over the concentration of defects [30, 31]. In (In, Mn)As grown by MOVPE a higher Curie temperature of 333 K has been reported [32, 33]. This result is not well understood since the Curie temperature is found to be independent of manganese concentration. Also, the magnetization has been measured in an applied field much larger than the coercive field [32, 33] so that fluctuations are strongly suppressed and the measured T_c is not the true transition temperature where spontaneous long-range order appears. In (Ga, Mn)N even higher Curie temperatures in excess of 750 K have been observed [34]. However, the failure to observe an anomalous Hall effect indicates that ferromagnetism and electronic conduction might take place in different phases.

In II–VI materials manganese is isovalent with the host cation so that it only provides a spin. The interplay of Coulomb attraction and exchange important for manganese in III–V compounds is thus missing here. Additional doping is required to introduce charge carriers. Manganese-doped II–VI semiconductors have been studied quite extensively [35, 36], mostly before the advent of III–V materials with high T_c. II–VI DMSs are typically not ferromagnetic but ferromagnetism has been achieved using modulation doping [37]. The Curie temperature does not exceed 2 K.

Regarding group IV semiconductors, only Ge has been successfully doped with magnetic ions, in this case manganese, resulting in Curie temperatures of up to 116 K [38]. This DMS is strongly insulating [38]. It is similar to III–V compounds in that manganese acts as a double acceptor, leading to a strongly p-type semiconductor.

Magnetically doped wide-gap oxide semiconductors have been predicted to show high Curie temperatures [39]. Matsumoto *et al* [40] have prepared $(Ti, Co)O_2$ with cobalt concentrations of up to 8%. Curie temperatures above 400 K have been estimated from the experiments [40]. Recent measurements of the anomalous Hall effect show that the carriers are strongly affected by the magnetic order [41]. However, oxide DMSs are still not well understood. A brief review can be found in [42].

For a DMS to order ferromagnetically there has to be an effective ferromagnetic interaction between the impurity spins, which is very probably carrier mediated for most or all ferromagnetic DMSs. This picture is supported by measurements of the anomalous Hall effect in (Ga, Mn)As [9, 10, 26], since the magnetization extracted from these experiments agrees reasonably well with that obtained from direct SQUID-magnetometer measurements [9, 10] and from magnetic circular dichroism [43]. This shows the intimate connection between carriers and impurity spins. Even more compelling evidence is obtained from electric field-effect experiments on (In, Mn)As [44, 45] and (Ga, Mn)As [46], in which the carrier concentration is altered by the application of a gate voltage in a field-effect-transistor geometry. The experiments show a very strong dependence of the coercive force on carrier concentration, besides a significant dependence of T_c.

In (Ga, Mn)As there is a metal–insulator transition between insulating samples with small manganese concentration and metallic samples with larger concentration. Insulating behaviour is here characterized by a diverging resistivity for $T \to 0$, indicating localization of carriers. Conversely, in metallic samples the resistivity decreases and eventually saturates for $T \to 0$. In this paper the term 'metal–insulator transition' refers to the quantum phase transition at $T \to 0$ and not to crossovers at finite temperature, as it is sometimes used in the DMS literature. It is important to note, however, that even for the most metallic samples the resistivities are relatively high, of the order of 10^{-3}–10^{-2} Ω cm [26, 47–49]. They are thus *bad metals*, showing that disorder is rather strong even in this regime.

We introduce a number of quantities for later use: we denote the concentration of magnetically active impurities by n_m. For III–V semiconductors with zincblende structure these are assumed to be substitutional impurities and in the absence of interstitial defects n_m is related to the doping fraction x, e.g., in $Ga_{1-x}Mn_xAs$, by $n_m = 4x/a_c^3$, where a_c is the length of the conventional cubic unit cell of the fcc cation sublattice. The *carrier fraction p* is the number of carriers per magnetically active impurity. This fraction is typically smaller than unity due to compensation. We refer to the charge carriers as *holes* to make the presentation more readable but the discussion also holds for electrons in the case of (largely hypothetical) n-type DMSs.

1.2. Types of impurity

As noted above, substitutional manganese in GaAs and most other III–V semiconductors (but not in GaN) forms a shallow acceptor state made up of valence-band states [17, 18]. The strong Coulomb–Hubbard interaction between the electrons in the d shell, $U \approx 3.5$ eV [50], leads to a large Mott–Hubbard splitting of the d states. Typically, *ab initio* calculations tend to find a significant d-orbital admixture close to the Fermi energy [24, 51–55]. This is at least partly due to the failure of the local-density or local-spin-density approximation to correctly describe this splitting. The consequence is that partially filled d bands are predicted to lie close to the Fermi energy. Recently, density-functional calculations using improved methods such as LDA + U [24, 56, 57] and self-interaction-corrected LSDA [58, 59] show less d-orbital weight in the relevant states, approaching a picture of valence-band-dominated impurity states. In (Ga, Mn)As both the occupied and the empty d states apparently end up far from the Fermi energy. Consequently, charge fluctuations in the d shell are suppressed, leaving only the spin

degrees of freedom, exchange coupled to the carrier spins [60]. Since the d shell is half filled, Hund's first rule predicts a local spin $S = 5/2$, in agreement with experiments [17, 18, 26].

The shallow-acceptor model for manganese in GaAs is discussed in detail in [61]. The 112 meV binding energy of an isolated manganese impurity level is made up of a larger contribution (86 meV) due to Coulomb attraction and a smaller contribution (26 meV) from the exchange interaction with the local manganese spin [61].

For the understanding of the spatial distribution of defects in DMSs it is important to check the mobility of substitutional manganese. While not much is known quantitatively, experiments on digital heterostructures [62, 63] show that part of the substitutional manganese moves several lattice constants during growth at 230 °C, without additional annealing. Vacancies may play a role in the diffusion of substitutional defects [48], lowering the energy barriers for this diffusion.

For DMSs grown by low-temperature MBE a high density of other defects is expected. Arsenic antisites are also known to occur in pure GaAs grown at low temperatures [64–67] and are also believed to be present in (Ga, Mn)As [9, 26, 68]. In low-temperature growth under arsenic overpressure, a high concentration of manganese is expected to lead to increased incorporation of the oppositely charged antisites [53, 69, 70]. This is supported by experiments [71, 72]. The antisite concentration strongly depends on the growth technique; when As_4 quadrumers are cracked to form As_2 dimers before they hit the DMS surface, the antisite concentration can be strongly reduced [30, 31, 49]. Conversely, in samples grown with an As_4-dominated flux [9, 26] the concentration of antisites is high and responsible for most of the compensation. The mobility of antisites is believed to be low [73] (see, however, [48] for a different view). Arsenic *interstitials* may also be present but have received little attention.

The situation is simpler in $Ge_{1-x}Mn_x$ since antisite defects cannot exist by definition so that compensation is most likely due to interstitial manganese. Apart from this fact, much of the discussion in this paper applies to $Ge_{1-x}Mn_x$ as well.

The third type of impurity important in manganese-doped DMS is manganese *interstitials*. The presence of interstitials has been proposed by Mašek and Máca [74] and demonstrated by channelling Rutherford backscattering experiments by Yu *et al* [75]. For a total manganese concentration corresponding to $x \sim 0.07$ about 17% of manganese impurities were found to be in interstitial positions [75]. Under the typical As-rich growth conditions, *ab initio* calculations predict a substantially lower energy of substitutional manganese defects compared to manganese interstitials [76, 77]. According to Erwin and Petukhov [76], a relatively large concentration of interstitials is nevertheless incorporated because close to the growing surface manganese positions that develop into interstitials in the bulk are energetically preferred.

There are two relevant non-equivalent interstitial positions: manganese may be in tetrahedral positions coordinated by four arsenic or four gallium ions (the hexagonal position is much higher in energy [55]). The arsenic-coordinated $T(As_4)$ position is locally similar to the substitutional position but the next-nearest-neighbour shell is very different. Intuition suggests that it should be lower in energy than the gallium-coordinated $T(Ga_4)$ position with its short cation–cation bonds [31]. *Ab initio* calculations indicate that it is indeed lower by 0.3 to 0.35 eV assuming charged interstitials [31, 78]. Interstitial manganese acts as an double donor. Also, according to [55, 75] subsitutional and interstitial manganese defects have the tendency to occupy adjacent positions due to their Coulomb attraction. The interstitial then occupies a $T(Ga_4)$ position. In this situation, the two impurity spins should interact *antiferromagnetically* due to superexchange. The strength of this interaction is at least -26 meV [55], leading to the formation of spin singlets that do not participate in ferromagnetic order. There is at present no agreement on the exchange interaction between $T(Ga_4)$ manganese spins and carrier spins. According to [79] the spin of the interstitial is nearly decoupled from the carriers, whereas

in [55] the interaction is found to be only a little smaller than for substitutional manganese. For the T(As$_4$) position, the interaction is practically the same as for substitutionals [55], reflecting the similar neighbourhood. Manganese interstitials are thought to be highly mobile [75] due to lower energy barriers for their motion as compared to substitutionals.

1.3. From isolated impurities to the heavy-doping limit

With increasing concentrations of magnetic impurities and holes there is a series of crossovers from first isolated impurities with weakly bound holes to an impurity band, which finally merges with the valence band. We discuss some important aspects of these crossovers in the following.

The magnetic impurities bind holes in hydrogenic impurity states. Due to the exchange interaction J_{pd} between hole spins and defect spins, the two spins align with each other at sufficiently low temperatures. In the case of Mn in GaAs, the exchange interaction is antiferromagnetic [9, 18, 61, 80]. The impurity-state wavefunction falls off roughly at the length scale of the Bohr radius a_B. To be more precise, the hopping integral between two ground-state (1s) wavefunctions reads [81]

$$T(R) = E_0 \left(3 + \frac{3R}{a_B} + \frac{R^2}{3a_B^2} \right) \exp\left(-\frac{R}{a_B} \right), \tag{1}$$

where E_0 is the binding energy of an isolated dopand. A central-cell correction has been neglected here. The hopping integral thus falls off to $1/e$ of its value at zero separation on a length scale of $\bar{a} = 2.394\, a_B$. To have only *a single* impurity in a volume of $\bar{a}^3$, the impurity concentration has to be relatively low, 1.536×10^{20} cm^{-3}, corresponding to $x = 0.7\%$ in (Ga, Mn)As, outside or perhaps at the border of the concentration range where magnetic order is observed. Thus typically a hole spin sees several impurity spins even in the insulating regime. This conclusion is not changed by spin–orbit coupling, although it has a significant effect on the impurity-state wavefunction and on the hopping integral [82].

If there are several acceptors in the range $\bar{a}$, it does not make sense to keep only the Coulomb attraction of one of them and neglect the others. In other words, the hole will not be in a hydrogenic impurity state centred at one acceptor but rather in a more extended molecular-orbital-like state. This has already been pointed out in [83]. Coming from low concentration, the first step is to take dopand *pairs* into account [84]. A description relying on hydrogenic impurity wavefunctions is of limited applicability for $x \gtrsim 0.7\%$. To make this argument more precise, one should calculate the width of the impurity band from such a model. The assumption of hydrogenic impurity states tends to overestimate this width [85, 86]. Hence, if the calculated width becomes comparable to the binding energy of the acceptor, the assumption becomes questionable.

It is energetically favourable for a localized hole spin to align (in parallel or antiparallel depending on the sign of J_{pd}) with all the impurity spins in the vicinity, forming a *bound magnetic polaron* (BMP). This leads to an effective *ferromagnetic* coupling between impurity spins. If the hole concentration were very small compared to the concentration of magnetic impurities, i.e., $p \ll 1$, at low temperatures the system would consist of isolated BMPs and additional isolated impurity spins in regions with exponentially small hole density [83, 87, 88]. In this regime no magnetic order is expected except perhaps at exponentially small temperatures but even there it may be destroyed by quantum fluctuations.

In real samples the hole concentration is smaller than the concentration of acceptors due to compensation, but typically not by more than one order of magnitude. Many theoretical papers assume a typical fraction of holes per manganese impurity in (Ga, Mn)As of 10% based
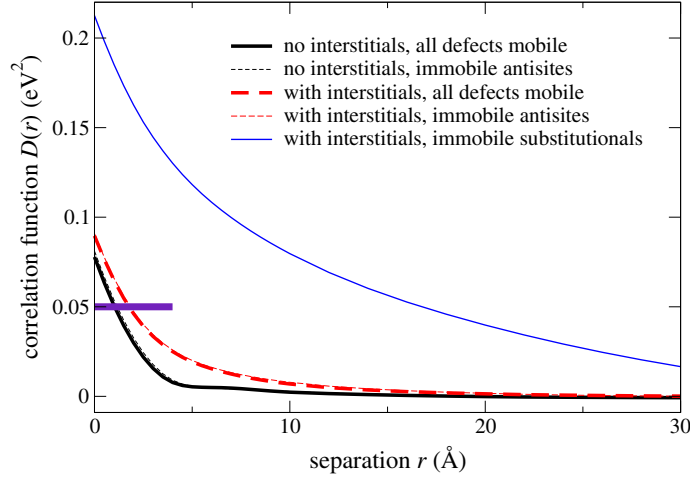
Figure 1. Correlation function $D(r)$ of the Coulomb disorder potential. All curves have been obtained performing sufficiently many MC steps to reach convergence, starting from a random distribution of defects at the appropriate sites in a supercell of $20 \times 20 \times 20$ conventional fcc unit cells (32 000 cations). Substitution of a fraction of $x = 0.05$ of cation sites (1600) by manganese and $p = 0.3$ holes per substitutional manganese ion have been assumed in all cases. For the curves marked 'no interstitials', compensation is entirely due to antisites (560 in this system) as in [69, 102, 103], whereas for the curves marked 'with interstitials', 20% of all manganese is in interstitial positions (corresponding to 400 interstitials and 160 antisites). The broad horizontal bar denotes the nearest-neighbour separation on the cation sublattice (3.9973 Å).

on earlier experimental papers [8, 26], but these estimates have been corrected upwards [9] and significantly higher values are now reached in any case [49]. In the case of (Ga, Mn)As, the concentration of antisites can be reduced by growing with As_2 dimers [30, 31, 49], as noted above. A hole fraction p above 90% was achieved for an Mn doping level of $x \approx 1.5\%$ [49].

Note that the *Kondo effect* [89, 90] is irrelevant for the DMS studied to date [91]. Kondo physics is relevant in the regime of large carrier concentration compared to the impurity concentration, $p \gg 1$. DMSs are so far always in the opposite regime of $p < 1$. However, in principle the DMS and Kondo regimes are continuously connected and it would be interesting to study the crossover to Kondo physics by increasing the carrier concentration, e.g., by codoping or even by application of a gate voltage.

For increasing impurity and hole concentrations the typical separation of holes eventually becomes of the order of $\bar{a}$. This happens for $pn_m\bar{a}^3 \sim 1$, i.e., $px \sim 0.7\%$ for (Ga, Mn)As. For strong compensation ($p \ll 1$) the corresponding impurity doping x is rather large. At this doping level the typical BMPs start to overlap. For higher concentrations a typical impurity spin has appreciable interaction with a number of hole spins. Of course, this interpretation only holds if it still makes sense to talk about carriers in individual hydrogenic impurity states. This can be checked using a theory that can describe both localized and extended states; see below.

In the band picture, isolated impurities are characterized by impurity levels. As the concentration of impurities is increased, some impurity states start to overlap. First, new impurity levels corresponding to close *pairs* of impurities will appear at energies depending on their separation [84]. At higher concentrations of magnetic impurities, these states merge into an impurity band. The width of this band increases with the impurity concentration. Most of the states in the impurity band are localized due to the disordered impurity positions.
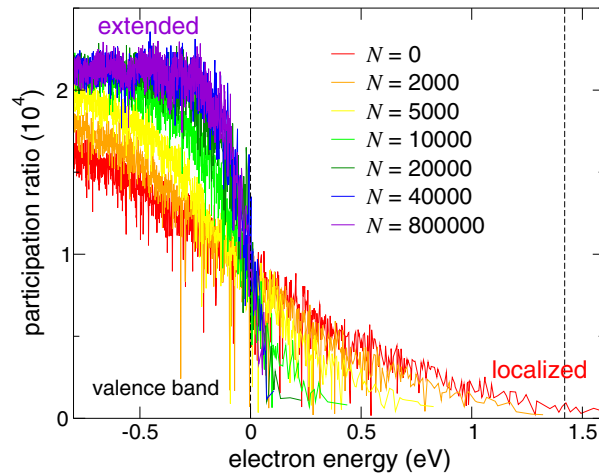
Figure 2. Participation ratio as a function of electron energy for $x = 0.05$ and $p = 0.3$ after various numbers N of MC steps increasing from the flattest to the steepest curve, after [102]. Zero energy is at the unperturbed valence-band edge.
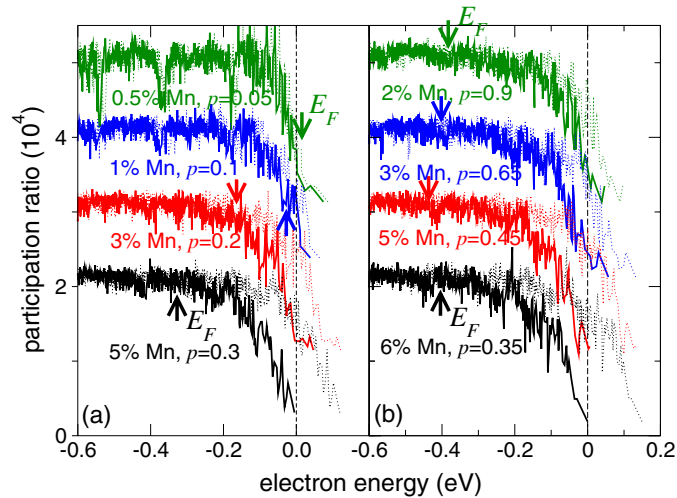

Figure 3. Participation ratio as a function of electron energy for various parameters x and p given in the plot, (a) for the (Ga, Mn)As samples of [9, 26], after [69], (b) for the samples of [49]. All impurity configurations have relaxed to thermal equilibrium in the MC simulation. For the exchange splitting full magnetization of manganese spins has been assumed. The Fermi energy is in each case indicated by an arrow.

Eventually the impurity band merges with the valence band and loses its independent character. In this heavy-doping limit the attractive Coulomb potential of the dopands is often neglected in the literature. Then the DMS is described in terms of holes in the valence band, which only interact with the impurities through their exchange interaction. This physics is described by the Zener model [39, 92–94] discussed in section 3.1.

However, there is no need to ignore the Coulomb interaction with the defects in a model starting from holes doped into the valence band. An acceptor introduces a hole and provides an

attractive Coulomb potential. If the impurity level is shallow the dopands can be well described in an envelope-function formalism [12]. To obtain the correct numerical value of the binding energy one has to include a phenomenological central-cell correction [61], which models the stronger Coulomb attraction of the hole to the impurity nucleus at short distances. Such a model reproduces the isolated bound impurity state but is applicable in the *entire* doping range up to heavy doping. It can thus, in principle, be employed to decide when (a) the picture of weakly interacting hydrogenic impurity states and (b) the neglect of the Coulomb disorder potential for valence-band holes are justified. Such an approach is applicable if there is no strong admixture of d orbitals of the magnetic impurity to the hole states [17, 18].

1.4. CPA versus supercell calculations

Finally, we discuss possible ways to include impurities in theories of DMSs. There are two basic approaches: first, one can consider a relatively large section of the lattice with many impurities and periodic boundary conditions. If this *supercell* is sufficiently large, one can capture disorder effects such as weak localization. This approach allows us to investigate the dependence of observables on system size, which allows us to use finite-size scaling to determine the localization length of states. It also allows us to treat not only fully random disorder but also impurities with correlated positions. We will see in section 2 that such correlations appear naturally in DMSs. The supercell approach can be used, in principle, in both *ab initio* and model theory, but quickly becomes very costly for *ab initio* calculations. For this reason it has mostly been applied to a supercell with a single substitutional manganese impurity; a concentration of $x = 0.0625$ already requires a supercell of 32 atoms. At present, supercells large enough to capture disorder effects do not seem feasible in *ab initio* approaches.

The second approach consists of the dynamical coherent-potential approximation (CPA), which treats the carriers as independent particles in an effective medium [95–99]. In the dynamical CPA this medium is described by a spin-dependent *purely local* self-energy $\Sigma_\sigma(\omega)$, which is determined from the CPA condition that the averaged carrier T-matrix vanishes [99]. The average here consists of both a spatial average over all sites, taking into account that some of them are occupied by impurities, and a thermal average over the orientations of impurity spins. The CPA includes multiple elastic scattering off a single impurity but not inelastic scattering. The CPA does not describe localization effects and is thus limited to the metallic regime. Since it is an effective-medium approach it cannot be used to study effects of the spatial distribution of defects. It is difficult to treat scattering potentials in CPA that are not purely local. This has been done in other condensed-matter systems [100] but not, to the author's knowledge, in DMSs. On the other hand, the CPA allows us to change the doping level continuously and does not require the use of a large supercell. It is thus also suited for *ab initio* calculations. A comparison of *ab initio* results obtained with the CPA and for a supercell is given in [53].

2. Properties of disorder

Due to the relatively low carrier concentration, electronic screening is rather weak and Coulomb interactions are correspondingly strong. From nonlinear screening theory [101] one obtains a screening length of

$$r_\mathrm{s} = \frac{(3n_\mathrm{m} - 2n_\mathrm{h})^{1/3}}{n_\mathrm{h}^{2/3}} = \left(\frac{3 - 2p}{4xp^2}\right)^{1/3} a_\mathrm{c}. \tag{2}$$

In (Ga, Mn)As, where $a_\mathrm{c} = 5.653$ Å, the screening length is $r_\mathrm{s} = 108.1$ Å for $x = 0.01$, $p = 0.1$ and $r_\mathrm{s} = 28.9$ Å for $x = 0.05$, $p = 0.3$. In the weak-doping limit the nonlinear

screening theory becomes inapplicable, though [101]. The screening length is thus larger than the typical length scale $\bar{a}$ of the hopping integral and the separation between impurities. Also, because of the $x^{-1/3}$ dependence of r_s we expect r_s to remain larger than this separation, as long as nonlinear screening theory remains valid. Furthermore, due to compensation, typically many defects of either charge are present. Consequently, neighbouring defects typically experience a nearly unscreened Coulomb interaction.

Let us first turn to the Coulomb disorder potential. Typically several charged defects are present within a sphere of radius r_s. Most papers that consider the microscopic defect positions at all assume a random distribution. However, the weakly screened Coulomb interaction makes a random distribution of defects very costly in energy. We expect two effects that reduce the Coulomb energy: firstly, during growth impurities are not incorporated randomly but in partially correlated positions, in particular due to the attraction of oppositely charged defects [53, 70]. Secondly, defect diffusion [48] leads to a rearrangement of defects that is energetically more favourable. In [69] the resulting impurity distributions are studied in the extreme case where the defects approach thermal equilibrium with respect to the Coulomb interaction. In [102, 103] the approach towards equilibrium during annealing is also considered. The compensation is assumed to be due to antisites. In the following, these results are briefly reviewed and a number of new results are presented.

In [69], Monte Carlo (MC) simulation of charged manganese substitutionals and arsenic antisites in (Ga, Mn)As at a typical growth and annealing temperature of 250 °C is used to obtain configurations close to equilibrium. The holes enter through the nonlinear screening length r_s [101]. The resulting equilibrium distribution is assumed to be quenched at low temperatures. The density of antisites is determined by charge neutrality from the manganese and hole concentrations estimated from experiment [9, 26, 49]. The main result is that for all realistic manganese and antisite concentrations the impurities arrange themselves in *clusters*, which typically contain oppositely charged manganese and antisite defects at nearest-neighbour positions on the cation sublattice. The cluster formation leads to a reduction of the Coulomb potential. For example, an antisite defect (charge +2) with two manganese impurities (charge -1) at nearest-neighbour positions is electrically neutral and only has a dipole or quadrupole field at large distances. Interestingly, Lee *et al* [13] suggest that *intentional* clustering of magnetic impurities will be used to produce functional heterostructures of DMSs. Note that a short-range attraction between substitutional manganese has been found in *ab initio* calculations [104, 105]. This chemical effect is not included in [69], but it would be easy to modify the potential accordingly.

Scanning tunnelling microscopy for (Ga, Mn)As with low doping, $x = 0.6\%$, does not show clear signs of clusters [71, 106]. However, this method is only sensitive for impurities within the topmost two layers. On the other hand, the experiments do show a significantly larger abundance of features attributed to defect pairs than expected for a random distribution [106]. It would be interesting to repeat these experiments for samples with large x.

Quantitative information on the Coulomb disorder can be obtained from the correlation function

$$D(r) \equiv \langle V(r)V(r')\rangle_{|r-r'|=r} - \langle V\rangle^2 \tag{3}$$

of the Coulomb disorder potential $V(r)$. Obviously, $\Delta V \equiv \sqrt{D(0)}$ is the width of the distribution of $V(r)$. Defect clustering has two effects: it strongly reduces $D(r)$ (and thus ΔV) and it makes $D(r)$ short-range correlated. While the reduction of ΔV is substantial, ΔV is still *not* small compared to the Fermi energy [69] even in the heavy-doping regime so that disorder cannot be neglected. As shown in figure 1, in equilibrium $D(r)$ decays to only about 10% of $D(0)$ on the scale of the nearest-neighbour separation. Thus $D(r)$ is well

approximated by a delta function. This initial decay is due to the screening of the compensated manganese impurities [102, 103]. Clearly, *ionic screening* by charged impurities is nearly perfect. The remaining uncompensated manganese ions cannot be screened by antisites and their contribution decays on a larger length scale determined by their density.

In (Ga, Mn)As antisite defects are believed to be immobile at typical growth and annealing temperatures [73]. However, the mobility of antisites in nearly perfect GaAs may not be a good indicator for the mobility in heavily doped (Ga, Mn)As, for which there is often another impurity in the nearest-neighbour shell. It would be worthwhile to study the mobility of antisites and substitutional manganese experimentally. In any case, if the antisites are held fixed in the MC simulations, the correlation function $D(r)$ is practically unchanged; see figure 1. Since there are many more manganese impurities than antisites, the manganese ions can easily screen immobile antisites.

Fiete *et al* [82] also perform MC simulations for the positions of substitutional manganese impurities in weakly doped (Ga, Mn)As. The objective is to introduce some degree of correlations between defect positions, similarly to [69]. For large numbers of MC steps a nearly perfect body-centred cubic lattice of impurities is found. This is not surprising since no compensating defects are included, i.e., all impurities have the same charge. Compensating defects are necessary for cluster formation [69].

The next step necessary for a realistic description is the incorporation of manganese *interstitials* [75]. We have performed MC simulations similar to [69] including charged (+2) interstitials and assuming the onsite energy in the $T(Ga_4)$ position to be 0.3 eV higher than in the $T(As_4)$ position [31, 78]. Figure 1 shows that the width ΔV as well as the correlation length increase slightly due to interstitials, if substitutional manganese is assumed to be mobile, regardless of the mobility of antisites. This is partly due to the fact that the MC simulation minimizes the configuration energy including the different on-site energies of interstitials, whereas $D(r)$ is the correlation function of the Coulomb potential alone. The correlation length is still of the order of the nearest-neighbour separation, though.

Assuming *only* the interstitials to be mobile—probably an unrealistic assumption [62, 63], even though interstitials are the most mobile defects—and starting from a fully random distribution of substitutional manganese impurities, the interstitials move to positions close to two or more substitutionals. In equilibrium, most reside in $T(As_4)$ positions due to the lower onsite energy. The $T(Ga_4)$ sites are closer to the substitutionals and thus reduce the Coulomb energy, but this gain is overcompensated by the higher onsite energy. The correlation function in figure 1 decays much more slowly, similarly to the case of random defects. The reason is that the high concentration of substitutional manganese impurities cannot be effectively screened by the lower concentration of interstitials. Of course, results like this depend on details of the configuration energy and are to be interpreted with caution.

In [77], small clusters of three manganese defects are studied with a density-functional total-energy method. Clusters made up of two substitutional and one interstitial defects are found to be favoured due to their Coulomb attraction, in qualitative agreement with the above discussion. Of course, *ab initio* theory captures additional 'chemical' contributions to the energy not included in [69].

3. Effects of disorder on transport

In the present section the effect of disorder on electronic transport is discussed. Experimentally, the resistivity for $T \rightarrow 0$ is found to either saturate (metallic behaviour) or diverge (insulating behaviour). As discussed above, metallic behaviour is seen for higher concentrations of magnetic impurities and thus, more relevantly, higher carrier concentrations. A metal–insulator

transition is observed as a function of impurity concentration [9, 26]. Annealing at low temperatures for short times is found to make the samples more metallic [48], whereas longer annealing [48] or annealing at higher temperatures [107] has the opposite effect. This is consistent with the expectation that higher disorder makes the sample less metallic.

At higher temperatures, the resistivity shows a clear peak centred around T_c [9, 26, 47, 49, 107]. For samples far in the insulating regime, where the resistivity increases very strongly for $T \rightarrow 0$, this peak develops into a shoulder [26]. This feature is very robust; it even survives in ion-implanted samples, where the disorder is very strong and dominated by implantation damage [108].

The Fisher–Langer theory [109] relates the fluctuation corrections of the resistivity of ferromagnets to their magnetic susceptibility. For a susceptibility of Ornstein–Zernicke form it predicts an infinite *derivative* of ρ at T_c and a very broad maximum at higher temperatures [109] in good agreement with experiments for ferromagnetic *metals* but not for DMSs. To apply the theory [109] to DMSs, the magnetic susceptibility at large q should be obtained [110].

The physics of impurities discussed in section 1.2 is expressed by a Hamiltonian of the form

$$H = H_b + H_m - J_{pd} \sum_n S_i \cdot s(R_n), \tag{4}$$

where H_b and H_m contain terms concerning only carriers and impurity spins, respectively, and the last term describes the local exchange coupling between carrier and impurity spins. In principle, H_b contains not only the band structure of the host semiconductor but also the electron–electron interaction and the interaction of electrons with the disorder potential due to impurities. The electron–electron interaction is assumed to be partly incorporated in the band structure, e.g., on the Hartree–Fock level, and the remaining correlation terms are usually neglected in the DMS literature (they might be important, though [88]). For very strong doping the Fermi energy measured from the band edge is large compared to the width of the disorder potential. In this limit, Coulomb disorder from the impurities may be ignored. However, even for 5% manganese in (Ga, Mn)As this condition is not satisfied [69, 111], so that the omission of Coulomb disorder is a rather severe approximation.

While the Coulomb disorder potential is most important for the observed metal–insulator transition, the additional disorder due to the exchange interaction with impurity spins shifts the transition further towards higher carrier concentrations [112]. By aligning the impurity spins in an external magnetic field, this source of disorder can be reduced, leading to less scattering for higher fields and thus to a negative magnetoresistance [112]. The system can even be driven to the metallic side of the transition by an external field [113, 114].

3.1. Band picture

Unperturbed host carriers (zero disorder potential) with an exchange interaction with impurity spins are described by the *Zener model* [39, 92–94]. This model still contains disorder since the positions of impurity spins appear in equation (4). To obtain an analytically tractable theory, a *virtual crystal approximation* (VCA) is often made, whereby the discrete impurity spins are replaced by a smooth spin density [12, 39, 94, 115]. This may be valid since the Fermi wavelength λ_F is typically larger than the separation between impurity spins and a carrier-mediated interaction automatically averages over length scales of the order of λ_F.

A simple way to restore some of the effects of disorder in the VCA is to assume a finite quasiparticle lifetime [111, 116–118]. The Coulomb and exchange contributions to this lifetime are estimated in [111]. The dominant Coulomb scattering leads to a quasiparticle width Γ of the order of 150 meV. This approach is only applicable in the strongly metallic regime since

it does not capture localization. The effect of $\Gamma > 0$ is clearly seen in theoretical results for the optical conductivity, where it leads to a broadening of the intraband (Drude) and interband peaks [116].

A related approach to the incorporation of disorder is employed in [110], where semiclassical Boltzmann equations are used to describe the dynamics of carriers and impurity spins, paying special attention to spin–orbit effects. The correlation function $D(r)$ of the Coulomb disorder potential can be assumed to be delta-function correlated [69]; see section 2. If $D(r) \approx \gamma \delta(r - r')$, the leading self-energy diagram yields the scattering rate $\hbar/\tau = 2\pi\gamma N(E_F)$ [4], where $N(E_F)$ is the electronic density of states per spin direction. The delta-function correlation also simplifies the description of scattering by collision integrals in the Boltzmann formalism. This approach yields analytical expressions for the carrier and impurity spin susceptibilities depending on the scattering rates from Coulomb and exchange disorder [110].

We now turn to approaches that treat the disorder potentials explicitly. Timm *et al* [69, 102, 103] study the hole states in the Coulomb disorder potential. The additional disorder due to the exchange interaction is small compared to the Coulomb disorder [111]. The impurity distribution is obtained from MC simulations. The envelope function and parabolic-band approximations are employed. For quantitative calculations the detailed band structure should be taken into account, e.g., using the six-band Kohn–Luttinger Hamiltonian [119–122]. The hole Hamiltonian is written in a plane-wave basis and diagonalized numerically, giving the energy spectrum and eigenfunctions $\psi_n(\mathbf{r})$. The normalized eigenfunctions determine the participation ratios [123]

$$\mathrm{PR}(n) = \left(\sum_{\mathbf{r}} |\psi_n(\mathbf{r})|^4 \right)^{-1} \tag{5}$$

of the states. (In part of the literature, including [69, 102, 103], this quantity is called the 'inverse participation ratio' but it seems more natural to follow [123] and call it the 'participation ratio'.) The participation ratio quantifies the number of lattice sites where the state n has a significant probability. Hence, the participation ratio scales with the system size for extended states but essentially remains constant for localized states. It thus allows us to estimate the position of the mobility edge in the valence band.

Figure 2 shows the participation ratio as a function of electron energy for $x = 0.05$ and $p = 0.3$, after various numbers of MC steps N [102]. The plot shows that for random defects ($N = 0$) the bandgap is filled in due to disorder, which is in contradiction to experiments. Thus correlated defects are required to explain the persistence of the energy gap. Finite-size scaling shows that the participation ratio in the flat region and the upper part of the slope scales with system size, whereas it become independent of system size in the band tail [102]. The mobility edge thus lies on the slope in figure 2. Since the MC simulation and also the diagonalization become numerically demanding for large system sizes, the finite-size scaling could not be carried out for sufficiently large systems to pinpoint the mobility edge exactly.

For the transport properties the states close to the Fermi energy are the most important. To find the position of the Fermi energy one has to take into account the splitting of the valence band by the exchange interaction. While the *disorder* due to this interaction is small, its *average* is not. The result is that for random defects the Fermi energy lies on the slope of the curve in figure 2, showing a strong tendency towards localization [69], whereas the states at the Fermi energy are extended for the 'annealed' (clustered) configuration. Thus in this model cluster formation is required to understand why (Ga, Mn)As with $x = 0.05$ is metallic. Figure 3 shows the participation ratio as a function of energy for parameters appropriate for (a) the samples measured by Matsukura, Ohno *et al* [9, 26] and (b) samples by Edmonds *et al* [49].

It is obvious that the shape of the curves does not change strongly, due to the strong ionic screening. In (a) the main effect is the shift of the Fermi energy due to the strongly changing hole concentration. The states at the Fermi energy are clearly extended for $x = 0.03$ and 0.05, while they are localized for 0.5% manganese [69]. This is in reasonable agreement with the experimentally observed metal–insulator transition [9, 26]. On the other hand, in (b) the Fermi energy hardly changes at all and stays well in the extended region, consistent with the experimental observation of metallic transport from $x = 1.65\%$ to 8.8% [49, 124].

Yang and MacDonald [88] extend this picture by not only including the Coulomb disorder potential due to substitutional manganese and antisites but also the Coulomb interaction *between holes*. Employing the Hartree–Fock approximation for the latter and considering the participation ratios, they also find metallic transport at $x = 0.05$ but insulating behaviour at $x = 0.0125$.

One can learn more by controlling the defect distribution by growing DMSs layer by layer. For example, in [62, 63] digital heterostructures consisting of half monolayers of MnAs separated by ten or 20 monolayers of GaAs are grown. The carrier concentration is systematically varied by codoping the GaAs layers with beryllium or silicon. All samples are insulating for $T \to 0$, consistent with strong disorder [63]. There are indications that part of the manganese diffuses out of the MnAs layers. The resistivity increases (decreases) if the hole concentration is reduced (inceased) by codoping [63]. We have performed MC simulations of the type of [69] for a superlattice of manganese-rich layers in GaAs. The number of MC steps has been chosen such that some interdiffusion occurs but the manganese-rich layers remain clearly defined. Diagonalization of the hole Hamiltonian than shows very strong smearing of the valence-band edge, more so than for a random distribution, and very small participation ratios (pronounced localization) of most states, in qualitative agreement with experiments [63].

Starting from a single-band model [125], Alvarez and Dagotto [126] calculate the density of states, optical conductivity and (magneto-)resistance of DMSs. The method [125, 126] relies on MC simulations for the orientations of classical impurity spins interacting with the holes. The model assumes a simple cubic lattice. The holes can visit any site but only a fraction of randomly selected sites carries impurity spins. Defect clusters are not studied. The Coulomb fields from charged impurities are neglected. This approximation is fairly restrictive since it removes the Coulomb disorder, only leaving the weaker disorder from the exchange interaction [111]. The hole Hamiltonian is diagonalized for each configuration of impurity spins during the simulation, which restricts the size of the supercell to at most 8^3 sites [125, 126].

For large J_{pd} the exchange interaction becomes strong enough to lead to weak localization of the holes [125, 126]. In the band picture, J_{pd} leads to the formation of impurity levels, which form an impurity band as the impurity states start to overlap. This is clearly seen in the density of states and, consequently, in the optical conductivity calculated in [126]. The DC resistivity is also evaluated in [126] using the Kubo formula. It shows metallic behaviour for small J_{pd} (weak disorder) and insulating behaviour for large J_{pd} (strong disorder). Interestingly, as seen in figure 4 (lower panel), for intermediate disorder strength the resistivity first increases with temperature up to $T \sim T_c$ and then decreases again [126], very similar to the experimental results. However, the model does not represent the situation realized in (Ga, Mn)As and probably most other DMSs, where the Coulomb interaction is the dominant origin of localization. Nevertheless the qualitative results should be valid regardless of the specific origin of localization.

The same model is studied within the CPA by Bouzerar *et al* [127, 128]. The Coulomb potential is omitted but a large exchange coupling J_{pd} leads to the formation of an impurity band [128], consistent with [125, 126]. For intermediate J_{pd} this band merges with the valence band.
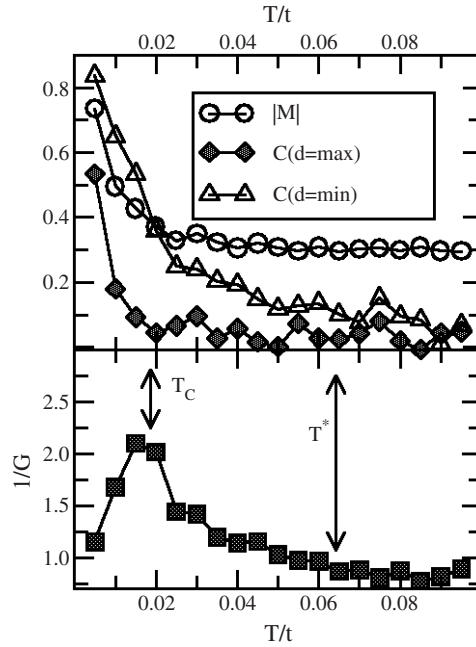
Figure 4. Upper panel: magnetization $|M|$ and spin–spin correlation function C from Monte Carlo simulations for a 12×12 lattice with 22 spins ($x \approx 0.15$) and 6 carriers ($p \approx 0.3$) and $J_{pd}/t = 1$, where t is the hopping amplitude in the tight-binding model. Lower panel: inverse of the conductance for the same model (from [126]).

3.2. Percolation picture

Kaminski and Das Sarma [83] consider the effect of disorder in the *localized* regime, conceptually starting from the light-doping limit. Similarly to other works [76, 82, 129–131] the main ingredients are holes in hydrogenic impurity states bound to magnetic acceptors. For *randomly* distributed impurities one obtains systems of overlapping BMPs [83, 87], as discussed in section 1.3. (We reserve the term 'clusters' for close groups of impurities.) At sufficiently low temperatures the impurity spins belonging to the same system are ferromagnetically aligned. If such a domain becomes infinite, long-range ferromagnetic order ensues. This is discussed further in section 4. For strongly localized holes [87], when the separation between acceptors is larger than the size of the impurity-state wavefunction, transport is due to thermally activated hopping of holes. Thus the resistivity diverges for $T \to 0$, showing insulating behaviour. On the other hand, no special signature is expected in the resistivity at the Curie temperature [83], essentially because *all* holes contribute to the resistivity, not only those in the infinite ferromagnetic domain forming at T_c. For $T \lesssim T_c$ this domain only comprises a small fraction of the sample volume, and only for holes moving within this domain the activation energy is reduced by ferromagnetic alignment [83, 131]. In addition, the contribution of the exchange interaction to the hopping activation energy is small compared to the Coulomb interaction. As discussed in section 1.3, the picture of strongly localized holes only applies for small doping levels. While the numerical results rely on the presence of *hydrogenic* impurity states, the conceptual picture also applies to impurity states more strongly localized due to d-orbital admixture.

Fiete *et al* [82] derive the parameters of a BMP model from a Kohn–Luttinger Hamiltonian restricted to heavy and light holes in the spherical approximation, i.e., all band energies depend

only on the modulus of the wavevector, a model introduced earlier in [132]. Due to spin–orbit coupling, the impurity-state wavefunction is not spherical [82]. The overlap between impurity states leads to the formation of an impurity band with a roughly symmetrical density of states. Employing finite-size scaling, Fiete *et al* [82] show that the states in the band tails are localized whereas they are extended in most of the band. For a manganese concentration of $x = 0.01$ the Fermi energy is found to lie just on the extended side of the mobility edge. The metal–insulator transition is concluded to take place in the impurity band [82].

How does this picture change if the magnetic impurities form *clusters* [83]? If several holes are present in the same cluster the total energy is increased due to their Coulomb repulsion. For an isolated impurity state this repulsion should be of the same order as the impurity-state binding energy so that double occupancy can be ignored. For a sufficiently large cluster, on the other hand, the charging energy becomes low enough to allow more than one hole to be present [83]. The system is still insulating since the resistivity is now controlled by the small hopping amplitudes *between* clusters. However, now a maximum in the resistivity is expected close to T_c [83]. Its origin is that now the clusters are ferromagnetically polarized well above T_c, which is also determined by the small hole hopping amplitudes between clusters. Thus at T_c already a significant volume fraction becomes ferromagnetically aligned, unlike in the previous case. Then a significant fraction of the holes experience a smaller activation energy due to the (nearly) optimal alignment of impurity spins [83]. Also, the exchange interaction can be expected to play a larger role now, since the Coulomb interaction is reduced for the more extended wavefunctions. These effects may lead to the observed decrease of the resistivity below T_c.

4. Effects of disorder on magnetic properties

Experimentally, an anomalous shape of the magnetization curve $M(T)$ is observed in DMSs [10, 28, 30, 38, 43, 48, 107, 108, 133–136]. From measurements of the temperature-dependent magnetization and comparison with various theories one can hope to learn more about DMSs and the role of disorder in particular [91]. In insulating samples the magnetization curve is often *concave* over a broad temperature range [38, 43, 108, 135, 136], i.e., $d^2 M/dT^2 > 0$. In metallic samples the magnetization curve is usually nearly linear over a broad range [10, 43, 135]. These results are in striking contrast to the Brillouin-function-like behaviour predicted by the mean-field theories of Weiss and Stoner [90] and observed in most insulating and metallic ferromagnets, respectively. The origin of the anomalous $M(T)$ is most likely that disorder is much more important in DMSs. In some samples the deviation from Brillouin-function-like behaviour is less pronounced [30, 48], presumably related to sample quality. The magnetization measured in an applied field of the order of or larger than the coercive field typically also follows a Brillouin function [32–34, 49]. Due to the applied field, fluctuations are suppressed, leading to a more mean-field-like curve.

4.1. Band picture

We return to the Hamiltonian in equation (4) describing carriers and impurities coupled by a local exchange interaction. Progress has been made employing the VCA and decoupling the exchange interaction at the mean-field level. Several authors [39, 94, 115] have rederived variants of the expression of Abrikosov and Gor'kov [138] for the mean-field Curie temperature,

$$k_B T_c = \frac{S(S+1)}{3} \frac{J_{pd}^2 n_m \chi}{g^2 \mu_B^2}, \tag{6}$$

where n_m is the impurity density, χ is the carrier spin susceptibility, g is the carrier g-factor and μ_B is the Bohr magneton. For a single parabolic band, an approximation more appropriate

for the conduction band than for the valence band, χ is just the Pauli susceptibility [90] $\chi_P = N(E_F)g^2\mu_B/2$, where $N(E_F)$ is the density of states per spin direction at the Fermi energy. Then the Curie temperature becomes $k_B T_c = S(S+1)N(E_F)J_{pd}^2 n_m/6$ [91]. It depends on the atomic fraction x of substitutional magnetic impurities and on the fraction of carriers per impurity as $T_c \propto p^{1/3}x^{4/3}$. Thus the increase of x should lead to higher Curie temperatures [39, 121]. However, growth of DMSs is typically limited to small x.

The term H_m in equation (4) contains a short-range antiferromagnetic superexchange interaction [137] between the impurity spins. In DMS this interaction is small compared to the ferromagnetic interaction, especially in (Ga, Mn)As [11, 39, 121]. Taking into account (a) the ferromagnetic Stoner-type interaction between the carriers, which increases the Curie temperature, and (b) the superexchange, which reduces T_c, one obtains the expression [11, 39, 121]

$$k_B T_c = \frac{S(S+1)}{6} A_f N(E_F) J_{pd}^2 n_m - k_B T_{AF}, \qquad (7)$$

where A_f is a Fermi-liquid parameter describing Stoner enhancement and T_{AF} is the correction due to superexchange. The mean-field Curie temperatures of various III–V, II–VI and group IV semiconductors doped with a fixed atomic fraction of manganese have been calculated by Dietl *et al* [11, 39, 121]. T_c strongly increases for lighter ions for two reasons: firstly, the factor n_m increases for smaller ion radii. Secondly, the effective masses and thus the density of states typically increase for semiconductors made up of lighter elements. On the other hand, the exchange interaction J_{pd} does not change strongly within each class (III–V, II–VI) of semiconductors [121]. The trend in T_c qualitatively agrees with experiments. However, in the case of (Ga, Mn)N, for which a Curie temperature above room temperature is predicted [11, 39, 121] and observed [34], the theory is of limited validity since manganese forms a deep acceptor level.

Magnetization curves of (Ga, Mn)As have been calculated from this mean-field theory by König *et al* [139], Dietl *et al* [121] and Das Sarma *et al* [91], among others. For large hole concentration a Brillouin-function-like shape of the impurity magnetization is found. For smaller carrier concentration the curves cross over to a concave shape over a broad temperature range [91, 121]. On the other hand, the (much smaller) hole contribution is also Brillouin-function-like for large hole concentration and becomes even steeper, with saturation at higher T/T_c, for smaller hole concentrations [91]. Kennett *et al* [140] generalize the VCA/mean-field theory to incorporate a *distribution* of exchange couplings J_{pd}. They show that a bimodal distribution of the effective fields experienced by the carriers makes the concave shape of the impurity-spin magnetization curve even more pronounced [140].

While the mean-field theory discussed so far assumes a *static* and homogeneous effective field, leading to a static and homogeneous self-energy of the carriers, the *dynamical mean-field theory* (DMFT) [141] drops the assumption of a static field. Thus quantum fluctuations are partially included. The DMFT has been applied to DMS by Das Sarma and coworkers [91, 142, 143]. For small carrier concentrations n_h the Curie temperature is found to increase rapidly with n_h, similarly to the ordinary mean-field prediction, but for larger carrier concentration T_c saturates or falls off again. Also, only for small hole–impurity exchange interaction J_{pd} is the mean-field result $T_c \propto J_{pd}^2$ found, while T_c increases more slowly or even decreases for larger J_{pd} [142]. For the shape of the magnetization curves, the DMFT results essentially agree with those of ordinary mean-field theory [91]. The criticism can be put forward that the Coulomb potential of the acceptors is neglected in [142]. Thus the quantitative results concerning the formation of an impurity band, its merging with the valence band and the locatization of holes have to be interpreted with care.

4.1.1. Incorporation of disorder.   The approaches discussed at the beginning of this section neglect disorder. Disorder enters mainly in two ways: (a) the holes experience the Coulomb disorder potential of the charged defects and (b) the impurity spins are localized at the acceptor sites. The inclusion of the Coulomb potential is complicated by the weak screening. A simple approximation is to consider a *purely local* potential that depends on the type of impurity [144, 145]. It should be attractive for acceptors (unlike in [144]) and repulsive for donors. One should be careful in interpreting the results of such an approach, though. Any property that crucially depends on the special form of the potential, such as the density of states of an impurity band, is not easily generalized to real DMSs.

Takahashi and Kubo [145] consider (Ga, Mn)As in such an approximation, where a simple semicircular density of states is assumed for the valence band and compensating defects are neglected. The distribution of substitutional manganese is assumed to be random and the dynamical CPA is employed. For fixed impurity concentration $x = 0.05$ the Curie temperature is found to first increase with hole concentration, as in the VCA/mean-field approach, but then to decrease again and to vanish for small compensation $p = p_c \lesssim 1$ [145]. The decrease of T_c is an effect of the hole density of states, which for weaker doping can be understood from the properties of the impurity band: the width of the impurity band is found to increase with impurity spin polarization. Thus for small hole concentrations the hole energy is reduced in the ferromagnetic state, whereas for large concentrations the reduction is smaller and eventually becomes an increase, destroying ferromagnetism [145]. The authors [145] suggest that the same picture also applies for higher doping ($x = 0.05$). This mechanism is described as *double exchange*, not, as usual, in a narrow d band but in a narrow impurity band [145]. It should be checked how the results change for an impurity potential of longer range and with compensating defects included.

Disorder due to a weakly screened Coulomb potential and the distribution of impurity spins is studied in [69, 102, 103]. The Hamiltonian of holes in the Coulomb disorder potential is augmented by the exchange interaction with the impurity spins S_i ($S = 5/2$),

$$H = \sum_{n\sigma} \xi_n c_{n\sigma}^\dagger c_{n\sigma} - J_{\text{pd}} \sum_i s_i \cdot S_i, \tag{8}$$

where

$$s_i \equiv \sum_{n\sigma n'\sigma'} c_{n\sigma}^\dagger \psi_n^*(R_i) \frac{\sigma_{\sigma\sigma'}}{2} \psi_{n'}(R_i) c_{n'\sigma'} \tag{9}$$

are hole spin polarizations at the manganese sites [102]. ξ_n and ψ_n are the hole eigenenergies and eigenfunctions in the absence of exchange but including the Coulomb disorder potential. The Hamiltonian is decoupled in a mean-field approximation, where, importantly, no spatial average is taken. Details of the formal derivation within the functional-integral approach are given in [102]. The mean-field decoupling is very similar to the one employed in [129], which is, however, concerned with the light-doping regime. In [69, 102, 103] a *collinear* magnetization is assumed. One can show that the equations for T_c, obtained by linearizing the mean-field equations, are unchanged by dropping this assumption.

Figure 5 shows the magnetization curves for manganese and hole spins for $x = 0.05$ and $p = 0.3$ for random and equilibrium defect configurations [69, 102, 103]. Since these results are obtained from a mean-field theory for a disordered ferromagnet, one should not trust them at temperatures $T \sim T_c$. The shape of the impurity-spin magnetization curve is anomalous for random defects, showing a rapid initial decay and then a long linear region. The shape becomes convex and more Brillouin-function-like with annealing [69], except for a tail at higher temperatures. This qualitatively agrees with experimental annealing studies [48]. The anomalous shape for random defects is due to the localization tendency of the holes,
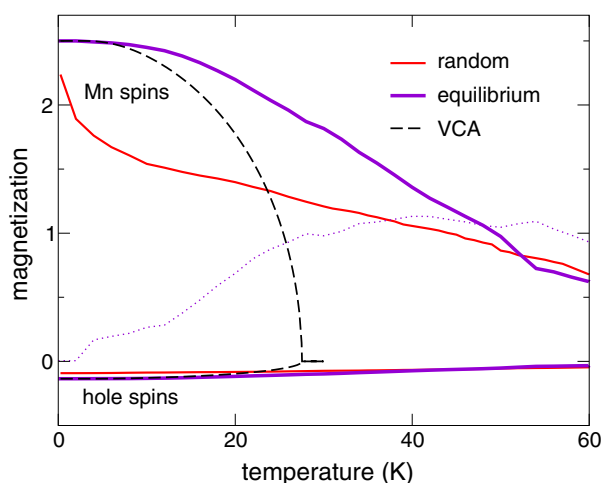
Figure 5. Magnetization of manganese (up) and hole spins (down) as functions of temperature for $x = 0.05$ and $p = 0.3$ for random and equilibrated (clustered) configurations, after [69, 102, 103]. The dotted curve gives the standard deviations of the manganese spin polarizations. For comparison, the long-dashed curves show the magnetizations obtained from a theory that totally neglects disorder.

which leads to a shorter-range effective manganese–manganese spin interaction and thus to a broad distribution of effective fields acting on these spins. For higher temperatures, only a few spins with strong interactions carry most of the magnetization, leading to a long tail for random defects. Figure 5 also shows the standard deviation of the manganese spin polarizations. The standard deviation becomes comparable to the average manganese spin polarization at intermediate temperatures. This shows that the decrease of the magnetization with increasing temperature is initially dominated by disordering of large moments and not by their reduction [102]. The hole-spin magnetization curve has a more normal shape. Note that the holes are not completely spin polarized at $T \rightarrow 0$ since the Fermi energy is larger than the effective Zeeman energy.

Figure 5 also compares the results with the disorder-free theory [39, 94, 115]. Note that the Curie temperatures are significantly *enhanced* by disorder. It is an important question whether this is an artefact of mean-field theory or a real physical effect. For random defect positions and correspondingly shorter-range manganese–manganese interactions, the mean-field T_c is governed by atypically *strong* couplings. (In the extreme limit, mean-field theory incorrectly predicts a nonzero T_c if only a single coupling is nonzero.) Thermal fluctuations destroy the long-range order in this case, reducing T_c. On the other hand, for clustered defects the hole states are extended, the effective manganese–manganese interactions are of longer range and mean-field theory is much more appropriate. Thus in the metallic regime the enhancement of T_c might be real.

It is also interesting that in $UCu_2Si_{2-x}Ge_x$, where *electronic* disorder is controlled by x whereas the magnetic uranium ions always form a regular lattice, T_c is enhanced by electronic disorder [146, 147]. Due to the coupling between impurity spins and carriers, disorder here leads to the damping of spin fluctuations which reduces their effect on T_c [146]. The same mechanism might also apply to the more complicated case of DMS [146, 147].

Mean-field magnetization curves obtained for various manganese concentrations and fully equilibrated defects [69, 102] show a crossover from a Brillouin-function-like shape at $x = 0.05$ to a concave shape at $x = 0.01$, as expected for insulating DMSs.
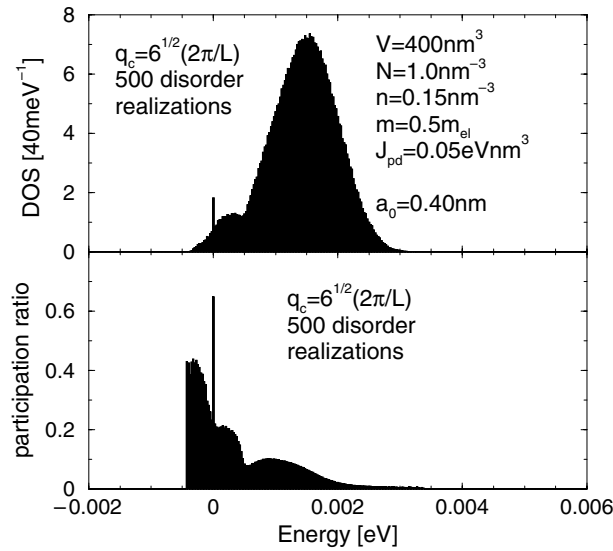
Figure 6. Density of states of collective magnetic excitations averaged over disorder realizations (upper panel) and averaged participation ratio of these states (lower panel). The participation ratio of the magnetic excitations can be interpreted as the fraction of spins that are actually taking part in an excitation. The sharp peak at zero energy corresponds to the Goldstone mode of uniform rotation of all spins. From [148].

Schliemann and MacDonald [148, 149] study the stability of the collinear mean-field magnetization. To that end they go beyond mean-field theory by deriving the spin-fluctuation propagator and from this the energies of elementary magnetic excitations, similarly to König *et al* [12, 139, 150]. However, in [148, 149] the disorder in the impurity positions is retained. The positions are assumed to be random. For a parabolic valence band it is shown that the collinear mean-field solution is stationary but that a fraction of the excitations generically appear at *negative* energies, as shown in figure 6 [148]. This means that the collinear saddle point is not stable. Figure 6 also shows that the modes with negative energy involve many impurity spins.

Similarly to the model of [125, 126], the Coulomb disorder potential is neglected in [148, 149] so that the localization properties of the holes are probably not correctly described. To take them into account, we can start from the model of [69], derive the mean-field approximation more formally using a Hubbard–Stratonovich decoupling and include Gaussian fluctuations in the decoupling fields. The details will be presented elsewhere [151]. The main result is apparent from figure 7: the excitations at negative energies persist if the Coulomb disorder potential is included, for both random and clustered impurities. It is also seen that the equilibration of defects and the corresponding reduction of disorder leads to a shift of weight to higher energies. This means that the magnetic system becomes *stiffer* with annealing, which is consistent with longer-range interactions. This stiffening has also been found by Singh [152].

While in [148] and in figure 7 a parabolic band is considered, the stability of the collinear state in the Kohn–Luttinger six-band model is studied in [149]. Whereas the collinear state is stationary but unstable for a parabolic band, it is not even stationary for the six-band model [149], i.e., in a collinear configuration a transverse *force* acts on the impurity spins. In particular, it is not the ground state. This is due to the interplay of spin–orbit coupling
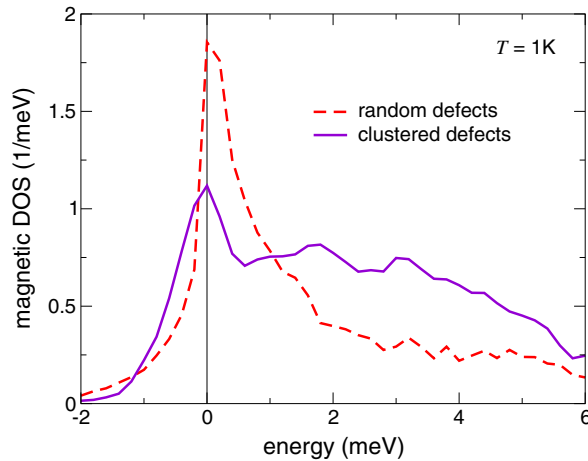
Figure 7. Density of states of magnetic excitations, assuming a collinear mean-field solution, calculated from the model of [69]. The dashed (solid) curve corresponds to the case of random (clustered) defects. The excitations are given a finite width of 0.1 meV to obtain smooth curves.

and disorder [149]. The deviation of the true ground state from collinearity may be small, though [153].

Another study of the effect of disorder has been presented by Chudnovskiy and Pfannkuche [154]. The model consists of holes on a lattice and impurity spins. A random number, taken to be five on average, of impurity spins is associated with every lattice site and assumed to have an exchange interaction with a hole at that site. Using a functional-integral approach and averaging over disorder with the replica trick, mean-field magnetization curves and estimates for T_c are calculated for various values of the *variance* of the number of impurity spins associated with each site [154]. Increased variance, i.e., stronger disorder, is found to lead to a higher Curie temperature [154]. However, the model is not easy to relate to real DMSs.

4.1.2. Beyond mean-field theory. It is important to check the applicability of mean-field theory. Schliemann *et al* [122, 155] perform hybrid MC simulations for holes interacting with classical impurity spins. They mostly consider a parabolic-band model but also a six-band Kohn–Luttinger Hamiltonian. The impurity spins are placed at fully random positions without regard of the lattice. The Coulomb disorder potential is neglected. A Gaussian form of the spatial dependence of the hole–impurity exchange interaction is assumed phenomenologically. We comment on this assumption in section 4.3. Unlike in [125, 126], the numerical effort due to the diagonalization of the carrier Hamiltonian is reduced by using a hybrid MC method, where all spins are updated at every step [122]. Up to 540 impurity spins are included. The Curie temperature is strongly reduced by fluctuations [122, 155]. Above T_c a phase with large local moments but no long-range order is found [122]. The magnetization curves for both impurity and carrier spins are found to be rather normal (Brillouin-function-like) for the parabolic-band case and slightly less so, with a nearly straight region, for the six-band model. The magnetization is generally not collinear for $T \rightarrow 0$, although this effect is rather small, especially for the six-band model [153]. For the parabolic band, the curves look very different from the mean-field results discussed above.

Alvarez *et al* [125, 126] also perform MC simulations for holes and classical impurity spins. The model has been discussed in section 3.1. The resulting magnetization curves are

quite anomalous for all parameters, nearly straight or concave in the whole temperature range up to T_c; see, e.g., figure 4 (upper panel) [125]. The origin of the discrepancy compared to Schliemann's work [122] is not clear. The tight-binding instead of parabolic band should not change the results qualitatively for the small Fermi seas considered here. The main technical differences seem to be

(a) that [122] allows the impurity spins to come arbitrarily close, whereas [125] contains a natural lattice cut-off for the separation, and

(b) that [122] treats much larger system sizes (up to 540 impurities compared to up to about 50 in [125]).

Whether the impurities sit on correct cation positions or are randomly distributed in the continuum does not seem to make an appreciable difference, though [149]. Further MC studies are definitely necessary, also to study the effect of clustered defects.

The dependence of T_c on J_{pd} is also discussed in [125]. For large J_{pd} the Curie temperature decreases since the exchange interaction becomes strong enough to localize the holes [125, 126], as discussed in section 3.1. If holes at the Fermi energy become localized a description in terms of percolation should become applicable.

4.2. Percolation picture

The application of the percolation picture to DMSs [76, 82, 83, 87, 91, 125, 129–131] extends earlier results for dilute ferromagnetic *metallic* alloys [156]. As discussed in section 1.3, the BMPs overlap for sufficiently high impurity and hole concentrations. This leads to an effective ferromagnetic interaction between impurity spins that are part of the same system of overlapping BMPs. At $T \rightarrow 0$ we expect a percolation transition as a function of impurity and hole concentrations, at which an infinite system of overlapping BMPs appears. Two BMPs are here said to overlap if the effective ferromagnetic interactions between the localized spins is so strong that their correlation is not destroyed by quantum fluctuations. To the best knowledge of the author, this quantum phase transition has not been studied to date. At finite temperatures, the ferromagnetic transition in this regime has been considered by Kaminski and Das Sarma [83, 87]. The main idea of this work is the following: the effective ferromagnetic interactions are inhomogeneous even for randomly distributed impurities. Therefore, at a given temperature $T > T_c$ only those impurity spins that are coupled by effective interactions that thermal fluctuations do not overcome will align ferromagnetically. In [83, 87] this physics is expressed by a temperature-dependent radius of BMPs. As the temperature is lowered, the size of the ferromagnetically aligned regions grows and eventually becomes infinite at T_c. The Curie temperature obtained by this percolation approach is [83, 87]

$$T_c \approx a_B \sqrt{n_m} n_h^{-1/6} s\, S |J_{pd}| \exp\left(-\frac{0.86}{a_B n_h^{1/3}}\right),$$ (10)

where s and S are the hole and impurity spin quantum numbers, respectively. For small hole concentration n_h the Curie temperature becomes exponentially small. Since quantum fluctuations are not included, T_c goes to zero only for $n_h \rightarrow 0$.

Essentially the same physics is discussed by Alvarez *et al* [125]. They denote the temperature where ferromagnetic domains form by T^*. For $T_c < T < T^*$ the magnetizations of the domains do not have long-range correlations. This is called a *clustered state* by Alvarez and Dagotto [157], who discuss this state as a special case of a more general paradigm that also applies to manganites and cuprates.

In the strongly localized regime the magnetization as a function of temperature has been obtained numerically using a mean-field approximation [129] and MC simulations [131] and

analytically within a percolation theory [87] and a mean-field approximation for localized holes [91]. In the numerical mean-field calculation the exchange interaction between hole impurity spins is decoupled at the mean-field level, while the disorder due to the (fully random) distribution of magnetic impurities is retained [129, 130]. This approach is limited to rather low doping [85, 86]. In [129, 130] the sign of the hopping integral (1) had to be inverted by hand to obtain reasonable results for the magnetization [85, 86]. Correcting the sign of $T(\mathbf{R})$ inverts the *highly asymmetric* impurity band, which drastically reduces the density of states at the Fermi energy, and, consequently, the mean-field Curie temperature [85]. This again indicates that a model with hydrogenic impurity states is not really sufficient.

The impurity magnetization curve of [129, 130] is concave over a broad temperature range, whereas the hole magnetization saturates quickly below T_c. The mean-field Curie temperature is found to be enhanced by disorder by a factor of about two relative to a periodic superlattice of manganese ions [129, 130]. These results are similar to the metallic regime discussed above. Since the effective interaction between impurity spins is of very short range here, the remark made there carries over: mean-field theory tends to overestimate T_c since it overemphasizes anomalously strong couplings. Thus the enhancement of T_c by disorder seems questionable in the localized regime [13]. In fact MC simulations performed for the same model [131] do not find a significant enhancement of T_c by disorder. The MC results for the magnetization curves also show an extended concave region but differ from the mean-field results in that they appear to stay concave up to T_c [131], similarly to MC simulations in the metallic regime [125].

In the MC simulations [131] the impurity magnetization for $T \rightarrow 0$ is much smaller than the saturated value. The origin discussed in [131] is that isolated impurity spins and small clusters are practically unoccupied by holes and do not order for any $T > 0$. However, even these impurity spins should experience an effective Zeeman field from the holes; the probability of finding a hole there is exponentially small but not zero. Thus for sufficiently small temperatures these impurity spins would come into alignment with the rest, but these temperatures might be unobservable in simulations and in experiments. Perhaps more relevant for real DMSs, quantum fluctuations—not included in the MC simulations—may destroy this order even at $T \rightarrow 0$.

The shape of both the impurity and hole magnetization curves from [129] is well reproduced by analytical results of the percolation [87] and mean-field [91] approach, indicating that the qualitative features of the magnetization are rather robust and do not depend on the details of the model [85]. Interestingly, the percolation theory [87] gives a *universal* expression for the magnetization, determined by the volume of the infinite ferromagnetic domain. The concave shape of the impurity magnetization curve found in mean-field theories [91, 129] is probably not an artefact since MC simulations [131] and percolation theory [87] find a similar shape, even though the actual value of T_c is strongly overestimated by mean-field theory [88, 139]. The concave shape becomes less pronounced with increasing concentration of impurity spins [87]. These results are qualitatively similar to the ones obtained from the band picture, see section 4.1, and also to the case of dilute ferromagnetic metals [156].

The Curie temperature T_c is predicted to decrease for large exchange interactions J_{pd} [125]. One origin of this effect is that the holes become more strongly bound to the impurities due to this exchange interaction. Thus the overlap between BMPs is reduced, their effective exchange coupling is weakened and T_c decreases. As noted above, the holes are eventually localized if J_{pd} becomes sufficiently large, but this is not the dominant mechanism in DMSs.

For *clustered* magnetic defects the percolation picture [83, 125] naturally predicts the Curie temperature to be dominated by the weak effective coupling *between* clusters. The mean-field approximation [69, 129, 148, 149] becomes increasingly inaccurate for pronounced clustering

if the effective interaction between impurity spins is of short range. The reason is that in mean-field theory T_c is governed by anomalously strong couplings within the clusters, whereas the true T_c is determined by the *weak* coupling between clusters. The condition of short-range interactions is crucial; see the discussion for the metallic case above. Quantitative results from percolation theory for T_c or the temperature dependence of the magnetization in the clustered case do not seem to exist. However, one can expect that large ferromagnetically ordered domains exist at $T \gtrsim T_c$, which align at T_c [83]. This should lead to a more rapid increase of the magnetization below T_c than for uncorrelated impurities. The same qualitative result is found for clustered defects in the metallic regime (but for a different reason—the disorder potential is reduced by clustering); cf section 4.1.1.

For $T \gtrsim T_c$ the domains are easily aligned by an applied magnetic field. In this situation the weak inter-cluster coupling becomes irrelevant and the magnetization is dominated by the strong coupling within the clusters. This should lead to a Brillouin-function-like magnetization curve, as observed in some experiments [32–34, 49].

One important conclusion is that the crossover from a 'normal' magnetization curve to a concave one for decreasing carrier concentration or increasing localization is very robust. This agrees with the experimental observation that the magnetization curves change smoothly with growth parameters and annealing time [48, 135], and thus with disorder strength. The experimental and theoretical results indicate that the $T = 0$ metal–insulator transition is not accompanied by a magnetic transition. Conversely, due to this robustness, comparison of calculated magnetization curves with experiment is not sufficient to decide between various models or approximations.

4.3. Spin-only models

We now turn to disorder effects in *spin-only* models of DMSs. It is an attractive proposition to remove the carriers from the model and incorporate their effect into the interaction between impurity spins. In principle, this can be done by integrating out the carriers, e.g., in the functional-integral formalism [12, 139, 150]. Employing a parabolic-band model without disorder and neglecting three-spin and higher interactions, one obtains the standard Ruderman–Kittel–Kasuya–Yosida (RKKY) interaction [90], as shown, e.g., by Dietl *et al* [94]. The effective interaction J_{ij} between spins S_i and S_j is an oscillating function of their separation, which leads to frustration. The typical period of these oscillations is determined by the Fermi wavelength λ_F, which in DMSs is typically *larger* than the distance between impurity spins. Thus their interaction is dominated by the first, ferromagnetic section of the oscillations, making ferromagnetic long-range order possible. In the limit that the typical separation is small compared to λ_F, this leads to essentially the same T_c as given in equation (6) [94]. For a random distribution of defects, the antiferromagnetic interactions dominate for *some* of them. These align *antiparallel* to the total magnetization [158], which leads to a reduced magnetization for $T \to 0$. For clustered spins this effect probably becomes even stronger, since now the typical separations between clusters become important, which are larger than the typical separations between random impurities. For weak compensation, i.e., large $p \approx 1$, more and more spins are antiferromagnetically coupled, eventually leading to spin-glass behaviour instead of ferromagnetism. In addition, as König *et al* [12, 139, 150] point out, the Zeeman energy in the effective field is smaller than the Fermi energy but not necessarily negligible, so that one should take the hole spin polarization into account in calculating the RKKY interaction.

It is interesting that Kępa *et al* [159] found in inelastic neutron scattering experiments on the II–VI material (Ze, Mn)Te that only a model of *itinerant* carriers [94] is in rough agreement with the measured carrier contribution to the RKKY-like interaction. A BMP model of strongly

localized holes does not fit the data. This is the case although the samples are insulating at low temperatures [159]. Presumably, the localization length is larger than the typical range of the RKKY interaction.

Zaránd and Jankó [132] employ the Kohn–Luttinger Hamiltonian [119] for GaAs restricted to heavy and light holes in the spherical approximation. Integrating out the holes, they obtain the effective interaction between manganese spins [132]. The hole polarization by other impurities is neglected here, as is the Coulomb disorder potential. Thus no disorder is present in the hole Green function. The interaction shows the usual oscillations with distance and, more interestingly, a pronounced anisotropy: in the effective interaction

$$H_{\text{eff}} = -K_{\parallel}(|\boldsymbol{R}_1 - \boldsymbol{R}_2|)S_1^{\parallel}S_2^{\parallel} - K_{\perp}(|\boldsymbol{R}_1 - \boldsymbol{R}_2|)\boldsymbol{S}_1^{\perp} \cdot \boldsymbol{S}_2^{\perp}, \tag{11}$$

where $S_i^{\parallel}$ and $\boldsymbol{S}_i^{\perp}$ are the components of the impurity spin $\boldsymbol{S}_i$ parallel and perpendicular to $\boldsymbol{R}_1 - \boldsymbol{R}_2$, respectively, the exchange parameters $K_{\parallel}$ and $K_{\perp}$ are typically very different, often even in their sign [132]. This leads to frustration even in an ordered arrangement of impurity spins. The origin of the anisotropy is the spin–orbit coupling in the valence band; without spin–orbit coupling there would not be any coupling between directions in spin space ($\boldsymbol{S}_i$) and real space ($\boldsymbol{R}_1 - \boldsymbol{R}_2$).

In the second step, MC simulations are performed for a classical spin-only model containing the anisotropic effective interaction [132]. The manganese impurities are randomly distributed on the face-centred-cubic cation lattice. For $x = 0.05$ the impurity magnetization curve is nearly straight for lower temperatures and becomes concave close to T_c, in qualitative agreement with mean-field results and the MC simulations of Alvarez et al [125, 126]. The impurity spins are not collinear for $T \to 0$. On the contrary, the angle between individual spins and the average magnetization direction shows a broad distribution, in particular for large hole fraction p, as a consequence of disorder together with the anisotropic interaction.

These results have been criticized by Brey and Gómez–Santos [160], who find that the spin anisotropy of the effective impurity-spin interaction is always smaller than 5%. They employ a six-band Kohn–Luttinger Hamiltonian for GaAs without additional approximations. In particular, this means that the Fermi surface is far from spherical [39, 121], unlike in [132]. The second difference is that in [160] a phenomenological Gaussian form of the hole–impurity exchange interaction J_{pd} is assumed, whereas in [132] this interaction is purely local. The width of the Gaussian is chosen of the order of the nearest-neighbour separation, but the results are found to depend significantly on this width [160]. Due to the $\boldsymbol{k}$-space cut-off imposed by this width, the RKKY-like interaction is found to be nearly isotropic [160], despite the highly non-spherical Fermi surface. The validity of the Gaussian J_{pd} has to be checked.

Motivated by the apparent smallness of the anisotropy, a disordered Heisenberg model with isotropic (in spin space and real space) interactions is studied in [160]. The magnetization curves obtained by MC simulation are quite Brillouin-function-like, except at low temperatures, where they approach full polarization with a finite slope [160]. Because of the isotropic interaction, the magnetization is collinear for $T \to 0$. The results agree quite well with the MC simulations of Schliemann et al [122] for essentially the same model, including the Gaussian form of J_{pd}. However, in [122] the carrier Hamiltonian is diagonalized at every MC step, whereas in [160] the holes are integrated out first. The agreement supports the treatment in [160], but does not of course say anything about the applicability of the model. The magnetization curves do not agree with the anomalous results discussed above, indicating that the model underestimates the effect of disorder.

The magnetic collective excitations are also considered in [160]. Their density of states is obtained and averaged over impurity realizations. For the effective spin interaction calculated for a parabolic-band model, it shows excitations at negative energies, consistent with [148];

see figure 6. These are shifted to positive energies for a broader Gaussian J_{pd} [160], since this Gaussian damps the RKKY-like oscillations and thus reduces frustration. For the six-band Kohn–Luttinger Hamiltonian no excitations at negative energies appear [160], due to the finite width of J_{pd} together with the non-spherical Fermi surface. In those cases the collinear ground state is thus found to be stable. However, Schliemann [149] has shown that the collinear state is not stationary for the six-band model and thus cannot be the ground state. Taken together, these results suggest that the ground state weakly deviates from collinearity.

A problem of all spin-only models discussed so far is the neglect of disorder in the calculation of the RKKY-like effective spin interaction. Priour *et al* [161] assume a free-carrier RKKY interaction between impurity spins [90] but include the effect of electronic disorder and a finite mean free path by a phenomenological exponential damping factor. They also add an antiferromagnetic nearest-neighbour interaction and assume a random distribution of impurity spins. A mean-field approximation that keeps the spatial disorder [69, 129] is then used to obtain magnetization curves and T_c [161]. They find a crossover from convex to concave magnetization curves with decreasing cut-off length in the RKKY interaction [161]. The Curie temperature is strongly reduced relative to the VCA result [39, 94, 115] by a small cut-off length (strong disorder).

Zhou *et al* [162] consider classical disordered Heisenberg models with various functional forms of the interaction. The effect of anisotropy in spin space and of electronic disorder, which is described by the width of the distribution of coupling constants, is studied with extensive MC simulations, motivated by the results of Zaránd and Jankó [132]. Random distributions of impurity spins on the fcc cation sublattice are assumed. Anisotropy is found to be irrelevant for the magnetization at high temperatures and to lead only to a small reduction at $T = 0$, in contrast to [132], regardless of the form of the interaction (short range versus long range, RKKY-like versus purely ferromagnetic) [162]. On the other hand, the frustration due to an oscillating RKKY interaction leads to a large reduction of the magnetization at $T = 0$. The effect of electronic disorder is found to be rather weak, but the magnetization curves become less Brillouin-function-like and more linear for large disorder [162]. It should be kept in mind that electronic disorder is incorporated phenomenologically by a distribution of coupling constants, which is not claimed to be realistic in [162].

The next step is the incorporations of disorder at the CPA level. Bouzerar *et al* [128] employ the CPA for a one-band tight-binding model without Coulomb disorder potential to evaluate the RKKY-like interaction, taking into account that the impurity spins are located at manganese sites. The hole–impurity exchange interaction J_{pd} is assumed to be local. For increasing $|J_{pd}|$ the Curie temperature overshoots the disorder-free value and then rapidly drops to zero [128]. Since the CPA does not include localization, the origin cannot be localization of holes, unlike the case in [125, 126]. Rather, for large $|J_{pd}|$ the impurity band split off the valence band and the density of states at the Fermi energy vanishes. It is also shown that the sign of J_{pd} is important for T_c, while the disorder-free RKKY theory just gives $T_c \propto J_{pd}^2$ [128]. In [163], the RKKY-like interaction is evaluated for a more realistic band structure of (Ga, Mn)As obtained from an *ab initio* calculation with a CPA treatment of disorder (substitutional manganese and antisites). The Coulomb disorder potential is neglected. The resulting impurity-spin interaction remains ferromagnetic up to large separations, in contrast to, e.g., [132]. This is probably why fluctuations are not found to suppress T_c dramatically. The partly contradictory results on the RKKY-like interaction in metallic DMSs show that further work is necessary.

Erwin and Petukhov [76] derive a spin-only model in the opposite *weak-doping* limit. The effective impurity-spin interaction is calculated in second order in the hopping amplitude between hydrogenic impurity states. It falls off exponentially since the hopping amplitude does; see equation (1). Standard percolation theory [164] is then used to obtain an approximate Curie

temperature. Interestingly, T_c vanishes for zero compensation, i.e., one hole per impurity, since for ferromagnetically aligned hole spins the holes then cannot hop. However, it should be kept in mind that this approach is limited to the dilute regime.

A quite different approach towards a simpler effective model is to integrate out the *impurity spins*, not the carriers. This is done by Santos and Nolting [165] for a disorder-free Kondo-lattice model and by Galitski *et al* [166] for DMSs in the strongly localized regime. In the limit of strong compensation, the system consists of nearly isolated BMPs made up of a single carrier and several impurity spins; see section 1.3. Starting from the percolation picture [87] the impurity spins can be integrated out, leading to an effective Heisenberg model for BMPs [166]. The effective exchange interaction is always ferromagnetic but depends exponentially on separation, making the Heisenberg model strongly disordered. A random distribution of magnetic impurities is assumed [166]. It is then proved that the paramagnetic phase is a *Griffiths phase* [167, 168] in this model, i.e., the magnetization is a (weakly) non-analytic function of the external magnetic field due to rare extended magnetic domains. Much stronger Griffiths–McCoy singularities [169] are derived for the local dynamic susceptibility in the paramagnetic phase [166]. Indeed, Galitski *et al* [166] suggest that insulating DMSs may be an ideal system to study Griffiths effects. It would also be interesting to study the Griffiths–McCoy singularities as the DMS is tuned towards the metallic regime.

5. Conclusions

By now it has been widely recognized that disorder plays an important role in DMS, as the works discussed in this paper attest. The detailed distribution of defects (random versus clustered) is crucial, since it strongly affects both the Coulomb disorder potential and the additional disorder due to the positions of impurity spins. Some approaches have neglected disorder or included only the disorder due to the distribution of impurity spins. But for a realistic description of transport the inclusion of the dominant source of scattering, i.e., the Coulomb disorder potential, is crucial, even in the metallic phase. The same holds for the magnetic properties since the magnetism is carrier mediated, as is clearly shown by experiments.

A multitude of models have been proposed and are treated by a variety of methods. Practically all theoretical studies start from either a band model or from a model of isolated impurity states. It is important to note, however, that the band model can in principle describe not only the metallic but also the insulating regime if disorder is properly taken into account. It is thus the more general description.

The shape of the magnetization curve has emerged as a standard yardstick for theories of DMSs. However, the concave shape of the impurity magnetization curve is not *only* an effect of disorder, since it also appears for disorder-free models. It tends to be more pronounced if disorder is included, though. In this case the magnetization curves become more concave for less metallic or more insulating DMSs, regardless of the model and the approximations used. On the other hand, the strong enhancement of T_c by disorder predicted by mean-field theories for both metallic and insulating DMSs is *not* seen in MC studies. This indicates that it is really an artefact of mean-field theory, although the issue is not yet fully settled. Transport measurements are, in principle, better suited to learn about disorder in DMSs. The problem here is that theory is at present lacking behind experiment. For example, no generally accepted theory for the resistivity maximum around T_c exists.

We conclude with listing directions of research that could advance the theory of DMSs at the present stage: firstly, the nature of the impurity states in DMSs with typical impurity concentrations of a few per cent should be analysed in detail. Are they really hydrogenic? The answer is crucial for building valid models.

More detailed simulations of DMS growth, starting from a microscopic model and perhaps employing *ab initio* calculations of configuration energies, would be very useful to understand the formation of the various defect species during low-temperature MBE. Further improvements in *ab initio* methods are required with the goal of obtaining shallow, *hydrogenic* impurity states in the weak-doping regime. One can then hope to describe the crossover to the heavy-doping limit correctly and to reproduce the qualitative difference between, say, (Ga, Mn)As and (Ga, Mn)N.

Also, a CPA treatment of DMS with a proper screened Coulomb potential would be desirable. Up to now all CPA treatments suffer from the assumption of a purely local Coulomb potential.

The inclusion of *quantum* fluctuations would also be very useful, for example in quantum MC simulations. As discussed above, quantum fluctuations are expected to destroy any ferromagnetic order at low impurity concentration. Simulations would provide information about the corresponding quantum phase transition, presumably of percolation type, as a function of concentrations and strength of disorder.

Finally, a transport theory for DMSs is still missing. In particular, there is no agreement on the origin of the resistivity maximum close to T_c. More generally, a better understanding of other response functions besides the conductivity, such as the magnetic susceptibility, would be highly desirable. The response is expected to be strongly affected by disorder. Understanding the spin and charge transport and the optical response of DMSs might be the most challenging but, in view of possible applications, the most worthwhile goal.

Acknowledgments

References

[1] Wolf S A, Awschalom D D, Buhrman R A, Daughton J M, von Molnár S, Roukes M L, Chtchelkanova A Y and Treger D M 2001 *Science* **294** 1488
[2] Dietl T 2001 *Acta Phys. Pol.* A **100** (Suppl.) 139
    Dietl T 2002 *Preprint* cond-mat/0201279
[3] Bennett C H and DiVincenzo D P 2000 *Nature* **404** 247
[4] Lee P A and Ramakrishnan T V 1985 *Rev. Mod. Phys.* **57** 287
[5] Kramer B and MacKinnon A 1993 *Rep. Prog. Phys.* **56** 1469
[6] Imry Y 1997 *Introduction to Mesoscopic Systems* (Oxford: Oxford University Press)
[7] Wan X and Bhatt R N 2000 *Preprint* cond-mat/0009161
[8] Ohno H 1998 *Science* **281** 951
[9] Ohno H 1999 *J. Magn. Magn. Mater.* **200** 110–29
[10] Ohno H and Matsukura F 2001 *Solid State Commun.* **117** 179–86
[11] Dietl T and Ohno H 2001 *Physica* E **9** 185–93
[12] König J, Schliemann J, Jungwirth T and MacDonald A H 2003 *Electronic Structure and Magnetism of Complex Materials* (*Springer Series in Material Sciences* vol 54) ed D J Singh and D A Papaconstantopoulos (Berlin: Springer) pp 163–211 (*Preprint* cond-mat/0111314)
[13] Lee B, Jungwirth T and MacDonald A H 2002 *Semicond. Sci. Technol.* **17** 393–403
[14] Sanvito S, Theurich G J and Hill N A 2002 *J. Supercond.: Incorp. Novel Magn.* **15** 85–104
[15] Dietl T 2002 *Semicond. Sci. Technol.* **17** 377–92
[16] Pearton S J *et al* 2003 *J. Appl. Phys.* **93** 1

[17] Linnarsson M, Janzén E, Monemar B, Kleverman M and Thilderkvist A 1997 *Phys. Rev.* B **55** 6938
[18] Okayabashi J, Kimura A, Rader O, Mizokawa T, Fujimori A, Hayashi T and Tanaka M 1998 *Phys. Rev.* B **58** R4211
[19] Blinowski J, Kacman P and Dietl T 2002 *Proc. Materials Research Society Symp.* vol 690 (Pittsburg, PA: Materials Research Society) p F6.9.1 (*Preprint* cond-mat/0201012)
[20] Sapega V F, Moreno M, Ramsteiner M, Däweritz L and Ploog K 2002 *Phys. Rev.* B **66** 075217
[21] Kojima E, Shimano R, Hashimoto Y, Katsumoto S, Iye Y and Kuwata-Gonokami M 2002 *Preprint* cond-mat/0212276
[22] Dietl T, Matsukura F and Ohno H 2002 *Phys. Rev.* B **66** 033203
[23] Zunger A 1986 *Solid State Physics* vol 39, ed H Ehrenreich and D Turnbull (Orlando, FL: Academic) p 275
[24] Mahadevan P and Zunger A 2003 *Preprint* cond-mat/0309509
[25] Ruzmetov D, Scherschligt J, Baxter D V, Wojtowicz T, Liu X, Sasaki Y, Furdyna J K, Yu K M and Walukiewicz W 2003 *Preprint* cond-mat/0302013
[26] Matsukura F, Ohno H, Shen A and Sugawara Y 1998 *Phys. Rev.* B **57** R2037
[27] Seong M J, Chun S H, Cheong H M, Samarth N and Mascarenhas A 2002 *Phys. Rev.* B **66** 033202
[28] Ohno H, Munekata H, Penney T, von Molnár S and Chang L L 1992 *Phys. Rev. Lett.* **68** 2664
[29] Ohno H, Shen A, Matsukura F, Oiwa A, Endo A, Kutsumoto S and Iye Y 1996 *Appl. Phys. Lett.* **69** 363
[30] Ku K C *et al* 2003 *Appl. Phys. Lett.* **82** 2302
[31] Edmonds K W *et al* 2003 *Phys. Rev. Lett.* submitted
     (Edmonds K W *et al* 2003 *Preprint* cond-mat/0307140)
[32] Blattner A J and Wessels B W 2002 *J. Vac. Sci. Technol.* B **20** 1582
[33] Blattner A J and Wessels B W 2003 *Preprint* cond-mat/0310104
[34] Sonoda S, Shimizu S, Sasaki T, Yamamoto Y and Hori H 2002 *J. Cryst. Growth* **237–239** 1358
[35] Furdyna J K and Kossut J 1988 *Diluted Magnetic Semiconductors* (*Semiconductors and Semimetals* vol 25) (New York: Academic)
[36] Dietl T 1994 *Diluted Magnetic Semiconductors* (*Handbook on Semiconductors* vol 3B) ed T S Moss (Amsterdam: North-Holland) p 1251
[37] Haury A, Wasiela A, Arnoult A, Cibert J, Tatarenko S, Dietl T and Merle d'Aubigné Y 1997 *Phys. Rev. Lett.* **79** 511
[38] Park Y D, Hanbicki A T, Erwin S C, Hellberg C S, Sullivan J M, Mattson J E, Ambrose T F, Wilson A, Spanos G and Jonker B T 2002 *Science* **295** 651
[39] Dietl T, Ohno H, Matsukura F, Cibert J and Ferrand D 2000 *Science* **287** 1019
[40] Matsumoto Y, Murakami M, Shono T, Hasegawa T, Fukumura T, Kawasaki M, Ahmet P, Chikyow T, Koshihara S-Y and Koinuma H 2001 *Science* **291** 854
[41] Toyosaki H, Fukumura T, Yamada Y, Nakajima K, Chikyow T, Hasegawa T, Koinuma H and Kawasaki M 2003 *Preprint* cond-mat/0307760
[42] Fukumura T, Yamada Y, Toyosaki H, Hasegawa T, Koinuma H and Kawasaki M 2003 *Preprint* cond-mat/0305435
[43] Beschoten B, Crowell P A, Malajovich I, Awschalom D D, Matsukura F, Shen A and Ohno H 1999 *Phys. Rev. Lett.* **83** 3073
[44] Ohno H, Chiba D, Matsukura F, Omiya T, Abe E, Dietl T, Ohno Y and Ohtani K 2000 *Nature* **408** 944
[45] Chiba D, Yamanouchi M, Matsukura F and Ohno H 2003 *Science* **301** 943 (published online 10 July 2003, 10.1126/science.1086608)
[46] Nazmul A M, Kobayashi S, Sugahara S and Tanaka M 2003 *Preprint* cond-mat/0309532
[47] Hayashi T, Hashimoto Y, Katsumoto S and Iye Y 2001 *Appl. Phys. Lett.* **78** 1691
[48] Potashnik S J, Ku K C, Chun S H, Berry J J, Samarth N and Schiffer P 2001 *Appl. Phys. Lett.* **79** 1495
[49] Edmonds K W, Wang K Y, Campion R P, Neumann A C, Foxon C T, Gallagher B L and Main P C 2002 *Appl. Phys. Lett.* **81** 3010
[50] Okabayashi J, Kimura A, Mizokawa T, Fujimori A, Hayashi T and Tanaka M 1999 *Phys. Rev.* B **59** R2486
[51] Akai H 1998 *Phys. Rev. Lett.* **81** 3002
[52] Máca F and Mašek J 2002 *Phys. Rev.* B **65** 235209
[53] Bergqvist L, Korzhavyi P A, Sanyal B, Mirbt S, Abrikosov I A, Nordström L, Smirnova E A, Mohn P, Svedlindh P and Eriksson O 2003 *Phys. Rev.* B **67** 205201
[54] Kudrnovský J, Turek I, Drchal V, Mašek J, Máca F and Weinberger P 2003 *Preprint* cond-mat/0302441
[55] Mašek J and Máca F 2003 *Preprint* cond-mat/0308568
[56] Park J H, Kwon S K and Min B I 2000 *Physica* B **281/282** 703
[57] Kudrnovský J 2003 private communication

[58]   Schulthess T C 2003 unpublished
[59]   Filippetti A, Spaldin N A and Sanvito S 2003 *Preprint* cond-mat/0302178
[60]   Schrieffer J R and Wolff P A 1966 *Phys. Rev.* **149** 491
[61]   Bhattacharjee A K and Benoit à la Guillaume C 2000 *Solid State Commun.* **113** 17
[62]   Kawakami R K, Johnston-Halperin E, Chen L F, Hanson M, Guébels N, Speck J S, Gossard A C and
         Awschalom D D 2000 *Appl. Phys. Lett.* **77** 2379
[63]   Johnston-Halperin E, Schuller J A, Gallinat C S, Kreutz T C, Myers R C, Kawakami R K, Knotz H,
         Gossard A C and Awschalom D D 2003 *Phys. Rev.* B **68** 165328
[64]   Look D C 1991 *J. Appl. Phys.* **70** 3148
[65]   Liu X, Prasad A, Nishio J, Weber E R, Liliental-Weber Z and Walukiewicz W 1995 *Appl. Phys. Lett.* **67** 279
[66]   Lutz R C, Specht P, Zhao R, Lam O H, Börner F, Gebauer J, Krause-Rehberg R and Weber E R 1999 *Physica*
         B **273/274** 722
[67]   Staab T E M, Nieminen R M, Gebauer J, Krause-Rehberg R, Luysberg M, Haugk M and Frauenheim T 2001
         Phys. Rev. Lett. **87** 045504
[68]   Sadowski J and Domagała J Z 2003 *Preprint* cond-mat/0309033
[69]   Timm C, Schäfer F and von Oppen F 2002 *Phys. Rev. Lett.* **89** 137201
[70]   Mašek J, Turek I, Drchal V, Kudrnovský J and Máca F 2002 *Acta Phys. Pol.* A **102** 673
         Mašek J, Turek I, Drchal V, Kudrnovský J and Máca F 2003 *Preprint* cond-mat/0302176
[71]   Grandidier B, Nys J P, Delerue C, Stiévenard D, Higo Y and Tanaka M 2000 *Appl. Phys. Lett.* **77** 4001
[72]   Schott G M, Faschinger W and Molenkamp L W 2001 *Appl. Phys. Lett.* **79** 1807
[73]   Suezawa M 1990 *Int. Conf. on Science and Technology of Defect Control in Semiconductors (Yokohama, 1990)*
         vol 2, ed K Sumino (Amsterdam: North-Holland) p 1043
[74]   Mašek J and Máca F 2001 *Acta Phys. Pol.* A **100** 319
[75]   Yu K M, Walukiewicz W, Wojtowicz T, Kuryliszyn I, Liu X, Sasaki Y and Furdyna J K 2002 *Phys. Rev.* B **65**
         201303(R)
[76]   Erwin S C and Petukhov A G 2002 *Phys. Rev. Lett.* **89** 227201
[77]   Mahadevan P and Zunger A 2003 *Preprint* cond-mat/0309502
[78]   Sullivan J M and Erwin S C 2003 unpublished
[79]   Blinowski J and Kacman P 2003 *Phys. Rev.* B **67** 121204
[80]   Sanvito S, Ordejón P and Hill N A 2001 *Phys. Rev.* B **63** 165206
[81]   Bhatt R N 1981 *Phys. Rev.* B **24** 3630
[82]   Fiete G A, Zaránd G and Damle K 2003 *Phys. Rev. Lett.* **91** 097202
[83]   Kaminski A and Das Sarma S 2003 *Preprint* cond-mat/0307294
[84]   Bhatt R N and Rice T M 1981 *Phys. Rev.* B **23** 1920
[85]   Timm C, Schäfer F and von Oppen F 2003 *Phys. Rev. Lett.* **90** 029701
[86]   Berciu M and Bhatt R N 2003 *Phys. Rev. Lett.* **90** 029702
[87]   Kaminski A and Das Sarma S 2002 *Phys. Rev. Lett.* **88** 247202
[88]   Yang S-R E and MacDonald A H 2003 *Phys. Rev.* B **67** 155202
[89]   Kondo J 1964 *Prog. Theor. Phys.* **32** 37
[90]   Yosida K 1996 *Theory of Magnetism* (Berlin: Springer)
[91]   Das Sarma S, Hwang E H and Kaminski A 2003 *Phys. Rev.* B **67** 155201
[92]   Zener C 1950 *Phys. Rev.* **81** 440
[93]   Zener C 1950 *Phys. Rev.* **83** 299
[94]   Dietl T, Haury A and Merle d'Aubigné Y 1997 *Phys. Rev.* B **55** R3347
[95]   Velický B, Ehrenreich H and Kirkpatrick S 1968 *Phys. Rev.* **175** 747
[96]   Kubo K 1974 *J. Phys. Soc. Japan* **36** 32
[97]   Faulkner J S 1982 *Prog. Mater. Sci.* **27** 1
[98]   Ruban A V, Abrikosov I A and Skriver H L 1995 *Phys. Rev.* B **51** 12958
[99]   Takahashi M and Mitsui K 1996 *Phys. Rev.* B **54** 11298
[100] Atkinson W A, Hirschfeld P J and MacDonald A H 2000 *Phys. Rev. Lett.* **85** 3922
[101] Shklovskii B I and Efros A L 1984 *Electronic Properties of Doped Semiconductors* (Berlin: Springer)
[102] Timm C and von Oppen F 2002 *Physics of Semiconductors 2002: Proc. 26th Int. Conf. on the Physics of
         Semiconductors (Edinburgh, 2002)* ed A R Long and J H Davies (Bristol: Institute of Physics Publishing)
         H35
[103] Timm C and von Oppen F 2003 *J. Supercond.: Incorp. Novel Magn.* **16** 23
[104] van Schilfgaarde M and Mryasov O N 2001 *Phys. Rev.* B **63** 233205
[105] Raebiger H, Ayuela A and Nieminen R M 2003 *Europhys. Lett.* submitted
         (Raebiger H, Ayuela A and Nieminen R M 2003 *Preprint* cond-mat/0307364)

[106] Sullivan J M, Boishin G I, Whitman L J, Hanbicki A T, Jonker B T and Erwin S C 2003
      Preprint cond-mat/0307165
[107] Van Esch A, Van Bockstal L, De Boeck J, Verbanck G, van Steenbergen A S, Wellmann P J, Grietens B,
      Bogaerts R, Herlach F and Borghs G 1997 *Phys. Rev.* B **56** 13103
[108] Park Y D, Lim J D, Suh K S, Shim S B, Lee J S, Abernathy C R, Pearton S J, Kim Y S, Khim Z G and
      Wilson R G 2003 *Phys. Rev.* B **68** 085210
[109] Fisher M E and Langer J S 1968 *Phys. Rev. Lett.* **20** 665
[110] Timm C, von Oppen F and Höfling F 2003 *Phys. Rev.* B submitted
      (Timm C, von Oppen F and Höfling F 2003 *Preprint* cond-mat/0309547)
[111] Jungwirth T, Abolfath M, Sinova J, Kučera J and MacDonald A H 2002 *Appl. Phys. Lett.* **81** 4029
[112] Dietl T, Matsukura F, Ohno H, Cibert J and Ferrand D 2003 *Proc. NATO Workshop on Recent Trends in Theory
      of Physical Phenomena in High Magnetic Fields* ed I Vagner *et al* (Dordrecht: Kluwer) p 197 (*Preprint*
      cond-mat/0306484)
[113] Katsumoto S, Oiwa A, Iye Y, Ohno H, Matsukura F, Shen A and Sugawara Y 1998 *Phys. Status Solidi* b **205**
      115
[114] Ferrand D *et al* 2001 *Phys. Rev.* B **63** 085201
[115] Jungwirth T, Atkinson W A, Lee B H and MacDonald A H 1999 *Phys. Rev.* B **59** 9818
[116] Sinova J, Jungwirth T, Yang S-R E, Kučera J and MacDonald A H 2002 *Phys. Rev.* B **66** 041202
[117] Sinova J, Jungwirth T and MacDonald A H 2003 *Phys. Rev.* B **67** 235203
[118] Jungwirth T, Sinova J, Wang K Y, Edmonds K W, Campion R P, Gallagher B L, Foxon C T, Niu Q and
      MacDonald A H 2003 *Appl. Phys. Lett.* **83** 320
[119] Luttinger J M and Kohn W 1955 *Phys. Rev.* **97** 869
[120] Abolfath M, Jungwirth T, Brum J and MacDonald A H 2001 *Phys. Rev.* B **63** 054418
[121] Dietl T, Ohno H and Matsukura F 2001 *Phys. Rev.* B **63** 195205
[122] Schliemann J, König J and MacDonald A H 2001 *Phys. Rev.* B **64** 165201
[123] Edwards J T and Thouless D J 1972 *J. Phys. C: Solid State Phys.* **5** 807
[124] Gallagher B L 2003 private communication
[125] Alvarez G, Mayr M and Dagotto E 2002 *Phys. Rev. Lett.* **89** 277202
[126] Alvarez G and Dagotto E 2003 *Phys. Rev.* B **68** 045202
[127] Bouzerar G and Pareek T P 2002 *Phys. Rev.* B **65** 153203
[128] Bouzerar G, Kudrnovský J and Bruno P 2002 *Preprint* cond-mat/0208596
[129] Berciu M and Bhatt R N 2001 *Phys. Rev. Lett.* **87** 107203
[130] Berciu M and Bhatt R N 2001 *Preprint* cond-mat/0111045
[131] Mayr M, Alvarez G and Dagotto E 2002 *Phys. Rev.* B **65** 241202(R)
[132] Zaránd G and Jankó B 2002 *Phys. Rev. Lett.* **89** 047201
[133] Munekata H, Ohno H, von Molnár S, Segmüller A, Chang L L and Esaki L 1989 *Phys. Rev. Lett.* **63** 1849
[134] Tanaka M 1998 *J. Vac. Sci. Technol.* B **16** 2267
[135] Mathieu R, Sørensen B S, Sadowski J, Södervall U, Kanski J, Svedlindh P, Lindelof P E, Hrabovsky D and
      Vanelle E 2002 *Preprint* cond-mat/0208411
[136] Limmer W, Koeder A, Frank S, Glunk M, Schoch W, Avrutin V, Zuern K, Sauer R and Waag A 2003 *Preprint*
      cond-mat/0307102
[137] Anderson P W 1959 *Phys. Rev.* **115** 2
[138] Abrikosov A A and Gor'kov L P 1962 *Zh. Eksp. Teor. Fiz.* **43** 2230
      Abrikosov A A and Gor'kov L P 1963 *Sov. Phys.—JETP* **16** 1575 (Engl. Transl.)
[139] König J, Lin H-H and MacDonald A H 2000 *Phys. Rev. Lett.* **84** 5628
[140] Kennett M P, Berciu M and Bhatt R N 2002 *Phys. Rev.* B **65** 115308
[141] Georges A, Kotliar G, Krauth W and Rozenberg M J 1996 *Rev. Mod. Phys.* **68** 13
[142] Chattopadhyay A, Das Sarma S and Millis A J 2001 *Phys. Rev. Lett.* **87** 227202
[143] Hwang E H, Millis A J and Das Sarma S 2002 *Phys. Rev.* B **65** 233206
[144] Calderón M J, Gómez-Santos G and Brey L 2002 *Phys. Rev.* B **66** 075218
[145] Takahashi M and Kubo K 2002 *Phys. Rev.* B **66** 153202
[146] Silva Neto M B and Castro Neto A H 2003 *Europhys. Lett.* **62** 890
[147] Silva Neto M B, Castro Neto A H, Mixson D, Kim J S and Stewart G R 2003 *Phys. Rev. Lett.* submitted
      (*Preprint* cond-mat/0307328)
[148] Schliemann J and MacDonald A H 2002 *Phys. Rev. Lett.* **88** 137201
[149] Schliemann J 2003 *Phys. Rev.* B **67** 045202
[150] König J, Lin H-H and MacDonald A H 2001 *Interacting Electrons in Nanostructures* (*Springer Lecture Notes
      in Physics* vol 579) ed R Haug and H Schoeller (Berlin: Springer) p 195

[151] Timm C 2003 unpublished
[152] Singh A 2003 *Preprint* cond-mat/0307009
[153] Schliemann J 2003 private communication
[154] Chudnovskiy A L and Pfannkuche D 2002 *Phys. Rev.* B **65** 165216
[155] Schliemann J, König J, Lin H-H and MacDonald A H 2001 *Appl. Phys. Lett.* **78** 1550
[156] Korenblit I Ya, Shender E F and Shklovsky B I 1973 *Phys. Lett.* A **46** 275
[157] Alvarez G and Dagotto E 2003 *Preprint* cond-mat/0305628
[158] Gyorffy B L, Pindor A J, Staunton J B, Stocks G M and Winter H 1985 *J. Phys. F: Met. Phys.* **15** 1337
[159] Kępa H, Van Khoi L, Brown C M, Sawicki M, Furdyna J K, Giebultowicz T M and Dietl T 2003 *Phys. Rev. Lett.* **91** 087205
[160] Brey L and Gómez-Santos G 2003 *Phys. Rev.* B **68** 115206
[161] Priour D J, Hwang E H and Das Sarma S 2003 *Preprint* cond-mat/0305413
[162] Zhou C, Kennett M P, Wan X, Berciu M and Bhatt R N 2003 *Preprint* cond-mat/0310322
[163] Bouzerar G, Kudrnovský J, Bergqvist L and Bruno P 2003 *Phys. Rev.* B **68** 081203
[164] Ioselevich A S 1995 *Phys. Rev. Lett.* **74** 1411
[165] Santos C and Nolting W 2002 *Phys. Rev.* B **65** 144419
      Santos C and Nolting W 2002 *Phys. Rev.* B **66** 019901 (erratum)
[166] Galitski V M, Kaminski A and Das Sarma S 2003 *Preprint* cond-mat/0306488
[167] Griffiths R B 1969 *Phys. Rev. Lett.* **23** 17
[168] McCoy B M and Wu T T 1968 *Phys. Rev.* **176** 631
[169] Bray A J 1988 *Phys. Rev. Lett.* **60** 720